Impact of urea fertilization rates on nitrogen losses, productivity and profitability in East African sugarcane plantations

Joseph Tamale, Paolo Nasta, Sebastian Doetterl, John Hutson, Oliver van Straaten, Laban F. Turyagyenda, Peter Fiener

Angaben zur Veröffentlichung / Publication details:

Tamale, Joseph, Paolo Nasta, Sebastian Doetterl, John Hutson, Oliver van Straaten, Laban F. Turyagyenda, and Peter Fiener. 2024. "Impact of urea fertilization rates on nitrogen losses, productivity and profitability in East African sugarcane plantations." *Soil Use and Management* 40 (2): e13030. https://doi.org/10.1111/sum.13030.

Received: 23 March 2023 | Revised: 30 January 2024 | Accepted: 1 February 2024

DOI: 10.1111/sum.13030

Soil Use and Management | WILEY

RESEARCH ARTICLE

Impact of urea fertilization rates on nitrogen losses, productivity and profitability in East African sugarcane plantations

Joseph Tamale[1,2] | **Paolo Nasta**[3] | **Sebastian Doetterl**[4] | **John Hutson**[5] | **Oliver van Straaten**[6] | **Laban F. Turyagyenda**[2] | **Peter Fiener**[1]

[1]Institute of Geography, University of Augsburg, Augsburg, Germany

[2]Ngetta Zonal Agricultural Research and Development Institute (NGEZARDI), Lira, Uganda

[3]Department of Agricultural Sciences, AFBE Division, University of Naples Federico II, Portici, Naples, Italy

[4]Soil Resources, Department of Environmental Systems Science, ETH, Zürich, Switzerland

[5]College of Science and Engineering, Flinders University, Adelaide, South Australia, Australia

[6]Northwest German Forest Research Institute, Göttingen, Germany

Correspondence
Peter Fiener, Institute of Geography, University of Augsburg, Augsburg 86159, Germany.
Email: peter.fiener@geo.uni-augsburg.de

Funding information
Deutscher Akademischer Austauschdienst; Deutsche Forschungsgemeinschaft; International Foundation for Science, Sweden; National Agricultural Research Organization, Uganda

Abstract

Fertilizer-intensive sugarcane plantations are expanding in sub-Saharan Africa (SSA) amidst increased groundwater pollution and carbon footprint concerns. Yet, the impact of nitrogen (N) levels on N losses, productivity and profitability in these plantations remains unclear. To address this gap, we conducted a completely randomized design experiment in a Ugandan sugarcane plantation using three N fertilization rates (low, standard and high) as treatments. N leaching under the different treatments was determined using the average drainage fluxes across a 1-m-layered profile which we estimated with a suite of pedotransfer functions (PTFs) and leachate N concentrations from suction cup lysimeters. Soil nitrous oxide fluxes were determined using static vented chamber bases and gas chromatography. Partial factor crop productivity was estimated from the average field fresh weight under each treatment and the amount of N fertilizer applied, while the return on investment was determined from the factory price of the field fresh weight and the market price of fertilizers. Our findings indicate that three out of five PTFs effectively estimated soil hydraulic properties at our test site, based on the close match between measured and predicted soil matric potential values. Notably, N leaching at low and standard N rates were comparable but significantly lower than at higher-than-standard N rates. Additionally, we measured comparable soil nitrous oxide emissions and field fresh weight but partial factor productivity and return on investment declined along the fertilizer intensification gradient. In conclusion, the study demonstrates the promising application of certain PTFs in N-leaching modelling in the data-scarce SSA. Furthermore, obtaining comparable field fresh weight with minimal N losses at lower-than-standard N rates presents an opportunity to mitigate groundwater pollution and greenhouse gas emissions. However, the potential impact of the switch from standard to low N rates on soil organic carbon stocks and sugarcane yields warrants further investigation.

KEYWORDS

LEACHM, nitrogen leaching, nitrogen uptake, partial factor productivity, pedotransfer functions, sugarcane

1 | INTRODUCTION

Sugarcane (*Saccharum officinarum*) is an important source of sugar (Brumbley et al., 2008; de Morais et al., 2015; Singh et al., 2008) and biofuel (Carmo et al., 2013; Mello et al., 2014) in many (sub) tropical countries and accounts for nearly 1.75% (26.5 million hectares) of the world's arable land area (Leff et al., 2004). The ongoing debate on energy production suggests that the global dependency on fossil fuels and the associated greenhouse gas (GHG) emissions to the atmosphere can be significantly reduced if the bioenergy potential of crops like sugarcane is efficiently harnessed in large plantations (Bordonal et al., 2018; Popp et al., 2014). However, the shift from fossil fuel to bioenergy requires massive crop biomass production, which is mostly achieved through nitrogen (N) fertilization, with application rates ranging between 60 and 400 kg N ha^{-1} $year^{-1}$ for both freshly established and ratoon sugarcane crops (Meyer & Antwerpen, 2010; Robinson et al., 2011; Stewart et al., 2006; Tamale et al., 2022). Nonetheless, these rates often exceed standard crop N requirements even in the case of the deeply weathered and nutrient-poor Ferralsols (where most sugarcane crops are grown; Cherubin et al., 2015), resulting in significant N losses to the environment and atmosphere (Robinson et al., 2011; Tilman et al., 2002).

One pathway through which N is lost from fertilizer-based sugarcane systems is nitrate (NO_3^-) leaching (Blum et al., 2013; Ghiberto et al., 2011; Stewart et al., 2006; Thorburn et al., 2011), a process involving movement of applied N to the groundwater (Bijay-Singh & Craswell, 2021; Ju & Zhang, 2017; Zhou et al., 2016). Hence, N leaching represents both a serious contamination problem for drinking water and a large economic loss for these agricultural systems (Bijay-Singh & Craswell, 2021). It is for this reason that the last three decades have seen a surge in concerted scientific investigations to better understand the factors that underpin N leaching dynamics in fertilized sugarcane systems across tropical and subtropical regions (e.g., Japan; Okamoto et al., 2021, Australia; Stewart et al., 2006; Thorburn et al., 2011; Brazil; Blum et al., 2013; Ghiberto et al., 2011). These efforts included: (1) the use of tracers (such as ^{15}N-enriched fertilizer; Ghiberto et al., 2009; Meier et al., 2006) to quantify N loss via deep percolation and (2) the evaluation of process-based models (e.g., Leaching Estimation and Chemistry Model, LEACHM; Hutson, 2003, Agricultural Production Systems simulator, APSIM; Holzworth et al., 2014, HYDRUS; Šimůnek et al., 2008) for simulating water fluxes and N transport in the vadose zone under fertilized sugarcane (Shishaye, 2015; Thorburn et al., 2011).

Application of process-based models is underpinned by the availability of data on the climate, crop phenology and characteristics, depth to the water table and soil hydraulic properties (namely, the soil water retention function and hydraulic conductivity function; Nasta et al., 2021). However, soil hydraulic properties data are often lacking for most parts of sub-Saharan Africa. In such data-scarce regions, the use of pedotransfer functions (PTFs) to estimate soil hydraulic properties from readily available basic soil physical and chemical properties (i.e., grain size distribution, soil bulk density and organic carbon) is highly recommended (Nasta et al., 2021; Van Looy et al., 2017). Notwithstanding, PTF use in sub-Saharan Africa remains challenging because only a few region-specific PTFs exist (Aina & Periaswamy, 1985; Pidgeon, 1972) while the development of new ones is currently hampered by the lack of basic physical and chemical soil properties' data (Tomasella & Hodnett, 2004). Amidst these challenges, several studies reported successful application of existing PTFs (e.g., Rosetta; Schaap et al., 2001) developed for temperate zones to test sites outside their training and validation areas with satisfactory accuracy. For instance, Tombul et al. (2004) accurately predicted the hydraulic properties of sandy clay loam soils in a semi-arid basin in Turkey with Rosetta PTF and so did da Silva et al. (2017) for sandy soils in south-eastern Brazil. Whereas such findings provide promising prospects for PTF application in data-scarce regions, no single study, to date, has evaluated the suitability of temperate PTFs in predicting soil hydraulic properties in sub-Saharan Africa. Consequently, the scale of the N leaching problem under fertilized sugarcane systems in sub-Saharan Africa is poorly understood.

Besides N leaching, sugarcane plantations by virtue of the wet and humid tropical environments in combination with the relatively high N inputs, are considered significant anthropogenic sources of nitrous oxide (N_2O; Allen et al., 2010; Dattamudi et al., 2019; Wang et al., 2016). This greenhouse gas has a larger radiative forcing relative to carbon dioxide (Forster et al., 2007) and a strong depleting effect on stratospheric ozone (Ravishankara et al., 2009). It is estimated that nearly 2.2 kg N_2O-N ha^{-1} $year^{-1}$ is released globally from sugarcane plantations (Yang et al., 2021). However, such estimates still suffer from considerable uncertainty because their derivation is primarily premised on studies conducted in Australia (Allen et al., 2010; Wang et al., 2016) and Brazil (e.g., Carmo et al., 2013; Soares et al., 2015), with little to no representation of sub-Saharan Africa.

Despite the N losses, the sugarcane crop still recovers a proportion of the applied N in its biomass. However, the N recovery rates under sugarcane plantations are not fully reconciled with some studies reporting values between 20% and 40% (Antille & Moody, 2021; Meyer et al., 2007) while others reported values between 60% and 70% (Franco et al., 2011; Furtado da Silva et al., 2020). Consequently,

N utilization efficiency (or partial factor productivity) and return on investment under sugarcane remain poorly understood especially in the case of sub-Saharan Africa where studies on N losses, productivity and profitability in sugarcane plantations are rare. Hence, we conducted a study in a 5.6-hectare ratoon sugarcane field located in north-western Uganda with the following objectives:

1. To evaluate the feasibility of using five-well-established PTFs developed in Brazil, Europe and North America to predict the soil water retention and hydraulic conductivity functions for Ugandan Ferralsols. We hypothesize that Brazilian PTFs would be optimal predictors of soil hydraulic properties in Uganda compared with their temperate counterparts (European and American PTFs) because they were derived using a soil dataset that is morphologically and pedologically similar to our tropical test site soils.
2. To determine the effect of increasing N application rates (low, standard, high) on N losses (soil N leaching flux and soil N_2O fluxes). We hypothesize that soil N leaching losses and soil N_2O emissions will increase along the fertilizer intensification gradient (low < standard < high) because N fertilization will likely increase the available N in the soil beyond the plant and microbial N demands resulting in increased N losses via deep water percolation and (de)nitrification pathways.
3. To determine whether fertilizing below or above the standard N fertilization rates results in incremental productivity and profitability benefits for sugarcane farmers. We postulate that field fresh weight, crop N uptake, productivity and economic returns will likely increase along the fertilization intensification gradient (low < standard < high) potentially offsetting N losses due to soil N_2O emissions and leaching and thereby deliver increased economic returns for the farmers using higher-than-standard N rates.

2 | MATERIALS AND METHODS

2.1 | Study area description and available datasets

The study was carried out in a 5.6 hectare ratoon sugarcane field in Kanyege, north-western Uganda (1°41′37.9″ N, 31°30′6.3″ E, 1062 m a.s.l). The area is covered with large-scale sugarcane farms that supply raw materials to Kinyara Sugar Works Limited, the second-largest sugar processing company in Uganda. Atmospheric and weather data were obtained from: (1) an ATMOS 41 weather station (METER Group Inc, USA) installed 2 m above the ground in an open area at the study site. The weather station recorded precipitation, air temperature, wind speed, air relative humidity and net solar radiation at 15-min intervals between May 1, 2019 and June 30, 2020; (2) a weather station operated and maintained by the Uganda National Meteorological Authority (UNMA) located at 1°41′8.7″, 31°43′5.7″, 1146 m a.s.l about 27 km from the study site. We used data from the UNMA weather station for the period January 1 to April 30, 2019, before the installation of the ATMOS 41 weather station at the study site. UNMA weather data were recorded at an hourly temporal resolution. Potential evapotranspiration (ET_p) was estimated with the Penman–Monteith equation (Allen et al., 1998; Batsukh et al., 2021) using wind speed, air relative humidity, net solar radiation and minimum and maximum temperature data from ATMOS 41 and UNMA weather stations.

The mean annual rainfall over the study region is about 1700 mm and is distributed in two wet seasons (March to May and August to November) separated by an extended dry season between December and February and a short dry season in June and July (Lukwago et al., 2020). The mean annual temperature is approximately 25°C. The soils in the study area are well drained and deeply weathered (Tamale et al., 2022) and are classified as Petroplinthic/Pisoplinthic Rhodic Ferralsols (IUSS Working Group WRB, 2015). These soils were mainly formed from the weathering of Precambrian basement complex parent material consisting of granites and gneisses (Lehto et al., 2014). The static depth of the groundwater table ranges between 13 and 30 m below the ground level over the Masindi region (Nanteza et al., 2016). The study area has an undulating topography and ridge crests reaching a maximum altitude of 1150 m a.s.l (Conlong & Mugalula, 2001). While slopes in the study region can reach a maximum of 10%, the selected study site for the sugarcane experiment was relatively flat with slopes ranging between 1% and 3%.

2.2 | Experimental design

The study was conducted in a ratoon IV sugarcane field in Kanyege, north-western Uganda (Figure 1a,b). Ratooning entails harvesting the established sugarcane monocrop at maturity by cutting the aboveground biomass (stems and leaves) and leaving the roots and shoots to sprout in the next season and produce a new crop. Originally, the cane was planted in furrows by overlapping 5 cm ear-to-ear budded setts along the entire length of the furrow. At the same time, a 1.5 m spacing was maintained between furrows. The study follows the analysis of a completely randomized design (CRD; Tamale et al., 2022) experiment established at the beginning of February 2019. The CRD experiment consisted of 12 treatment plots laid out in a 5.6-hectare (ha) field. Each treatment plot measured 40 m × 40 m, had an inner

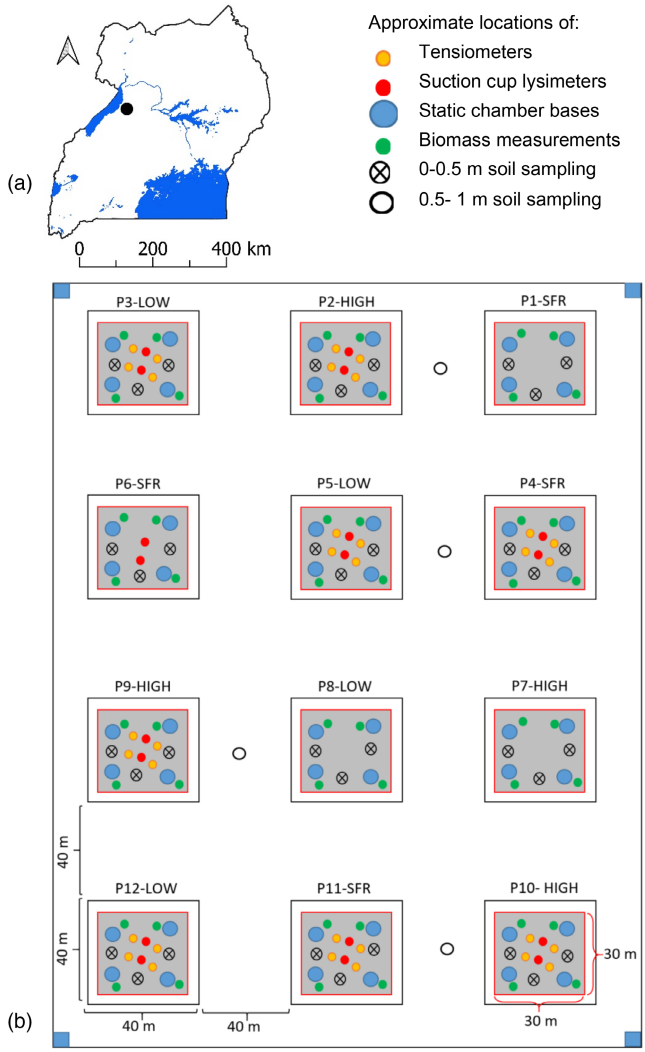

FIGURE 1 (a) Geographic location of the study area (black dot) in the north-western part of Uganda, (b) sketch of the completely randomized design (CRD) experiment set up in a 5.6 ha field. The CRD experiment consisted of 12 treatment plots (measuring 40 m × 40 m) in which soil matric potential, nitrate concentrations and soil nitrous oxide flux, were measured using tensiometers (yellow circles), suction cup lysimeters (red circles) and static chamber bases (blue circles), respectively, under standard (SFR; 70 kg ha^{-1}), low (0.5 times SFR) and high (1.5 times SFR) nitrogen (N) applications. The plots are labelled by reporting plot (P) number and four replications of N applications (LOW, SFR and HIGH). Biomass measurements (green circles) and soil sampling between 0 and 0.5 m depth (black crossed circle) were carried out in each treatment plot, while deep soil sampling (0.5–1.0 m; empty black circles) were located between the treatment plots.

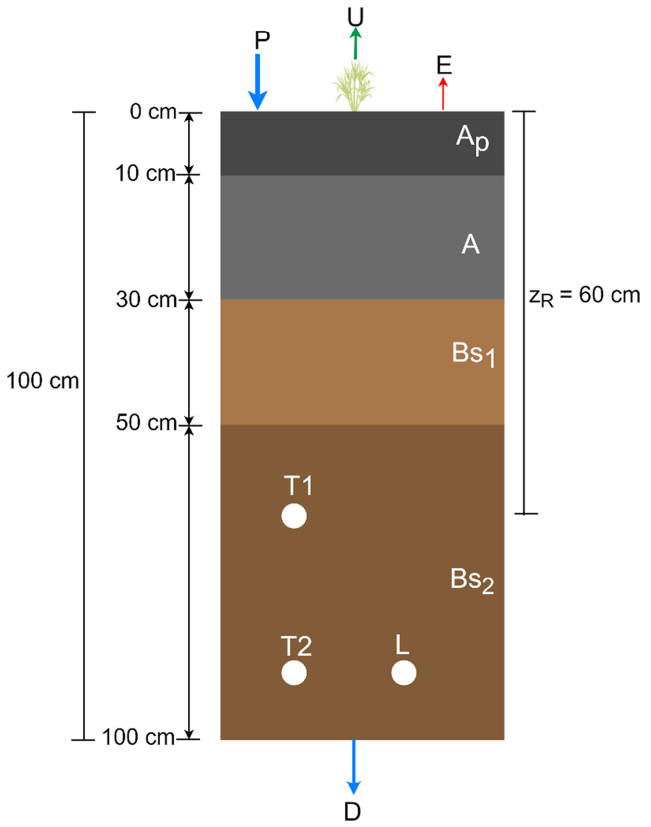

FIGURE 2 Sketch of the 1-m-deep soil profile composed of four soil layers (Ap, A, Bs_1, Bs_2 corresponding to 0–10 cm, 10–30 cm, 30–50 cm and 50–100 cm soil depths, respectively). Precipitation (P) and evaporation (E) occur at the soil surface. The sink term, U controls transpiration through the roots in the root zone ($z_R = 60$ cm) and water which moves across the bottom of the soil profile is lost by drainage (D). T1 and T2 are the observation nodes ($z = 60$ cm and $z = 90$ cm) at which simulated and measured matric potential values were compared to test the pedotransfer function performance. L is the location of the suction cup lysimeter in the layered soil profile.

measurement core of 30 m × 30 m to avoid boundary effects and was separated from adjacent plots by a 40 m guard row to prevent spillover of treatments (Figure 1b). The 12 experimental plots reflect three N fertilizer treatments (low, standard and high N applications) replicated four times ($n = 12$; three treatments × four replications). The standard fertilizer rate (SFR) of 70 kg N ha^{-1} applied as urea, $(NH_2)_2CO$ per crop growth cycle is the commonly used N application rate by sugarcane farmers in northwestern Uganda as per our interview with the key informant, Masindi District Sugarcane Growers' Association chairperson prior to the establishment of the experiment. In contrast, low and high N fertilizer rates were less common and referred to 0.5 and 1.5 times SFR, respectively. The fertilizers were applied to all treatment plots once on May 14, 2019 (at about 3 months from sprouting) in the 16-month growing cycle of the ratoon crops, following the standard practice by sugarcane farmers in the region (i.e., one-time N application at the surface without incorporation into the soil). For all treatments, inter- and intra-row weeding was done manually with a hand hoe three times during the first 8 months following sprouting, by which time the canopy was sufficient to subdue emerging weeds. The experimental activities illustrated in Figure 1 are explained in detail in Sections 2.3–2.5.

2.3 | Soil sampling

Disturbed and undisturbed soil samples were collected from three random locations in every replicate plot at three depths (0–10, 10–30, 30–50 cm; crossed circles in Figure 1b) and from deeper soil layers (50–100 cm; empty circles in Figure 1b) in four pits dug in the guard row spaces to minimize alteration to the soil-microenvironment within the inner measurement cores of the respective treatment plots. The sampling depths reflect the vertical variability of the soil profiles in which four soil layers were identified (Ap, A, Bs_1 and Bs_2; Figure 2). The disturbed soil samples were air-dried and sieved to 2 mm before being used for texture (sand, silt, clay) and soil organic carbon (SOC) content analyses. Grain size distribution was determined following the van Reeuwijk (1993) protocol. The protocol entails destruction of all organic matter in the soil samples using hydrogen peroxide solution followed by separation of the sand-sized particles (effective diameter from 0.05 to 2 mm) from the silt- (effective diameter from 0.002 to 0.05 mm) and clay-sized particles (effective diameter less than 0.002 mm; Gee & Or, 2002) by wet sieving while the silt- and clay-sized fractions were determined using the hydrometer method. The textural class of each soil sample was determined using the United States Department of Agriculture (USDA) classification and is coarse-textured (sandy clay to sandy clay loam) in the surface layers (0–30 cm) and predominantly fine textured (clay) in the subsurface layers (30–100 cm; Table 1).

Note, the collected soil samples contained no $CaCO_3$ and were, hence, considered free of inorganic C. SOC and soil organic nitrogen (SON) were determined with a C/N elemental analyser (vario EL cube; Elementar Analysis Systems GmbH, Hanau, Germany). Soil pH H_2O (1:2.5) was measured using a pH meter. Undisturbed soil samples were used to determine the soil bulk density ($g\,cm^{-3}$), defined as the oven-dry mass (>24 h at 105°C) per bulk volume (Kopecky ring, 251 cm^3). SOC and SON were multiplied by bulk density to obtain SOC- and SON-stocks, respectively, while accounting for the stone content.

2.4 | Overview of the temporal measurements

Temporal measurements included: (1) the estimation of drainage fluxes and (2) N losses under the different treatments.

2.4.1 | Estimation of drainage fluxes

Soil water drainage fluxes at the study site were estimated using the water subroutine of the Leaching Estimation and Chemistry Model (LEACHM; Hutson, 2003) by simulating the water flow across a 1-m-deep layered soil profile (Figure 2) representative of the 5.6 ha experimental area. The one-dimensional transient vertical water flow across the soil profile was modelled via a numerical solution of Richards' equation:

$$\frac{\partial\theta}{\partial t} = \frac{\partial}{\partial z}\left[K(\theta)\frac{\partial H}{\partial z}\right] - U(z,t) \quad (1)$$

where θ is the volume fraction of water ($cm^3\,cm^{-3}$), t is the time (d), z is the depth (cm), K is the unsaturated

TABLE 1 Mean (±standard error, SE; 4 ≤ N ≤ 36) basic soil physical and chemical properties at the soil depths of 0–10, 10–30, 30–50 and 50–100 cm based on measurements done at the experimental site (*N* denotes the number of soil samples).

	Soil depth (cm)			
Soil physico-chemical properties	**0–10**	**10–30**	**30–50**	**50–100**
Bulk density ($g\,cm^{-3}$)	1.08 ± 0.02	1.24 ± 0.02	1.20 ± 0.03	1.14 ± 0.03
Stone content (%)	4.0 ± 1.0	3.0 ± 0.9	4.0 ± 1.6	7.6 ± 3.3
Sand (%)	52 ± 2.2	47 ± 2.5	33 ± 1.5	29 ± 0.4
Silt (%)	21 ± 2.4	18 ± 2.0	13 ± 1.3	15 ± 5.4
Clay (%)	27 ± 1.1	35 ± 0.8	54 ± 1.5	56 ± 5.3
pH H_2O (1:2.5)	5.5 ± 0.1	5.5 ± 0.1	5.5 ± 0.0	5.4 ± 0.1
SON (%)	0.18 ± 0.0	0.14 ± 0.0	0.09 ± 0.0	0.06 ± 0.0
SOC (%)	2.7 ± 0.1	2.0 ± 0.0	1.1 ± 0.0	0.6 ± 0.0
C/N	14.8 ± 0.12	14.3 ± 0.13	11.7 ± 0.12	10.0 ± 0.13
SON stocks ($Mg\,N\,ha^{-1}$)	1.94 ± 0.04	3.39 ± 0.04	2.26 ± 0.05	3.67 ± 0.09
SOC stocks ($Mg\,C\,ha^{-1}$)	28.8 ± 0.7	48.6 ± 0.8	26.4 ± 0.8	36.6 ± 0.6

Note: SON and SOC indicate soil organic nitrogen and soil organic carbon, respectively.

hydraulic conductivity (cm d^{-1}), H is the hydraulic head (the sum of the pressure and gravitational soil water potential, cm) and U is the sink term representing absorption of water by plants (d^{-1}).

The root distribution was assumed to be uniform throughout the root zone ($z_R = 60$ cm; Figure 2). The surface boundary conditions were specified as precipitation (P), potential evaporation (E), while the bottom boundary condition was specified as unit-gradient drainage with an initial matric potential of −100 cm (D; Figure 2).

Soil water retention function was described using the van Genuchten (1980) equation, which relates the degree of saturation, S_e (−), to the soil matric potential, ψ (cm):

$$S_e(\psi) = \frac{\theta - \theta_r}{\theta_s - \theta_r} = \frac{1}{\left(1 + |\alpha\psi|^n\right)^{(1-1/n)}} \quad (2)$$

where θ_r ($cm^3\,cm^{-3}$) and θ_s ($cm^3\,cm^{-3}$) are the residual and saturated volumetric water contents, α (cm^{-1}) and n, (dimensionless) are the empirical shape parameters of the soil water retention function.

According to van Genuchten (1980), the hydraulic conductivity function is defined as:

$$K(S_e) = K_s S_e^{\tau}\left[1 - \left(1 - S_e^{\frac{1}{m}}\right)^m\right]^2 \quad (3)$$

where K_s (cm d^{-1}) is the saturated hydraulic conductivity, m is an empirical shape parameter (m = 1- 1/n) τ (−) is the tortuosity parameter usually assumed as either 0.5 (Mualem, 1976) or −1 (Schaap & Leij, 2000).

The soil hydraulic parameters (θ_r, θ_s, α, n and K_s) in each soil layer were estimated from the spatial-average of sand, silt, clay and soil bulk density values (Table 1) using five well-known PTFs developed in Brazil, Europe and North America. These PTFs included: (1) Rawls et al. (1982), (2) ROSETTA (Schaap et al., 2001), (3) Tomasella and Hodnett (1998), (4) Weynants et al. (2009), (5) Wösten et al. (1999), hereafter, denoted as RAWLS82, ROSETTA, T&H98, WEY09 and WOS99, respectively. Table A1 in the Appendix lists the equations of five PTFs (RAWLS82, ROSETTA, T&H98, WEY09 and WOS99) used to estimate the soil hydraulic parameters (θ_r, θ_s, α, n and K_s) featuring in the van Genuchten's soil water retention function (Figure A1) and hydraulic conductivity function (Figure A2).

Hence, we obtained five numerical simulations based on the five PTFs listed above. Next, we evaluated the performance of the five PTFs by comparing the match between simulated (PTF-based) and measured matric potentials using: (1) the coefficient of determination (R^2), (2) the index of agreement (d), (3) Nash–Sutcliffe efficiency (NSE) and (4) root mean square error (RMSE) indices. Soil matric potential measurements were obtained two to four times a month using two pairs of tensiometers (outer diameter = 16 mm, inner diameter = 12 mm; MMM tech support GmbH & Co. KG, Germany) installed at 60 and 90 cm depth in 8 of the 12 replicate plots of the CRD experiment. Hence, a total of 32 tensiometers were installed at the study site (yellow circles; Figure 1b). Optimal prediction is obtained with a value equal to zero for RMSE and equal to one for R^2, d and NSE. Measured and simulated values of soil matric potential on March 4 and March 9, 2020, were ignored because these measurements were close to the tensiometer's detection limit. Finally, the daily drainage flux was assumed as the mean of the daily drainage fluxes obtained with the best-performing PTFs.

2.4.2 | Nitrogen losses

The N losses under different treatments (low, standard and high) included: soil N leaching and soil N_2O emissions and are elaborated below.

Nitrogen leaching estimation

First, N concentrations in percolating water below the rooting zone were measured with suction cup lysimeters (outside diameter = 22 mm, interior diameter = 16 mm, wall thickness = 3 mm; MMM tech support GmbH & Co. KG, Germany). Before installation of the suction cup lysimeters, the effective rooting depth (z_R) for the sugarcane crop was determined. This involved digging nine 1.1 m depth pits in ratoon fields of varying ages (1.5 months ratoon 4, 8 months ratoon 9 and 15 months ratoon 4) and obtaining 10 soil monoliths in each pit measuring 20 cm in length, 20 cm in width and 10 cm in depth. The soil monoliths from each depth increment were placed on top of a 2 mm sieve and thoroughly washed in a basin full of clean water to separate the bulk soil from the root biomass. The roots were oven dried at 60°C for 48 h and weighed to determine the root biomass per depth increment. We established that over 90% of the roots in ratoon sugarcane fields were contained in the top 60 cm. Hence, z_R (60 cm) is the soil depth containing most plant roots (i.e., >90%). Therefore, the lysimeters were installed vertically at 90 cm soil depth (well below z_R) using a gouge auger whose diameter nearly matched the outer diameter (OD) of the lysimeter ceramic cup (OD = 22 mm) to ensure good capillary contact between the ceramic cup and the soil matrix. In addition, we obtained soil material closest to 90 cm depth, made it into a slurry and injected back the slurry into the drilling hole before installing the lysimeter. We, then heaped soil around the lysimeter shaft at the surface to prevent any preferential water flow along the shaft, which would potentially bias N concentration measurements at

the preferred depth. In total, we installed 18 suction cup lysimeters in nine treatment plots (one pair x nine plots; red circles; Figure 1b) but two suction cup lysimeters in plot 6 (P6-SFR) malfunctioned and we were unable to sample soil water from this plot. All suction cup lysimeters were installed 2 weeks before the first water sampling to ensure minimal alteration to the biochemical processes near the suction cup lysimeters. To capture the expected variability in soil water content due to crop root uptake, we installed one suction cup lysimeter in the inter-row space while the other one was installed in the intra-row space. A day before sampling, we applied a 40 kPa suction to the lysimeter using a hand vacuum pump for 24 h to collect adequate volumes of soil water. On the sampling day, the suction was released and the solution was collected from the lysimeter shaft using an airtight syringe. The collected water from the two-suction cup lysimeters in a plot was transferred to a pre-labelled plastic bottle and mixed thoroughly for about 30–60 s to obtain a homogeneous water sample for every plot. Each homogenized water sample was analysed for nitrate (NO_3^-) concentrations using a portable RQflex® 10 reflectometer test kit (Merck, Germany) equipped with a specific bar code and test strips (detection range: 0.3–90 mg N/L). Soil pore water sampling and NO_3^- leachate concentration determination were done once every 2 weeks for most of the sampling period. However, measurements were more frequent during the first month following fertilization (1 day before fertilization, three and 5 days after fertilization and then once a week until the end of the first month) to capture an expected NO_3^- flush in percolating water following N application.

Next, we applied a trapezoidal interpolation on the measured NO_3^- concentrations in percolating water to estimate the daily NO_3–N concentrations and afterwards multiplied by the mean daily drainage flux obtained with the best-performing PTFs (in LEACHM) in Section 2.4.1 to obtain the daily N leaching fluxes under the different treatments.

Soil nitrous oxide flux measurements

Soil nitrous oxide (N_2O) flux measurements from the respective treatments of the CRD experiment were reported in an earlier study by Tamale et al. (2022). Briefly, soil N_2O flux measurements involved randomly installing four static PVC chamber bases (area = 0.044 m^2, volume = ~12 L) at the soil surface (~0.03 m) within the inner measurement core of each treatment plot (blue circles; Figure 1b) a month prior to sampling (April 2019). On the sampling day, all chamber bases in each plot were covered with polyvinyl hoods (volume = 6.78 L) to obtain a pooled gas sample at each of four time intervals (3, 13, 23 and 33 min) using the approach proposed by Arias-Navarro et al. (2013). Soil N_2O fluxes were measured intensively in the first 6 months that followed fertilization and monthly for the remaining sampling period. The intensive soil N_2O flux measurements were to capture the expected soil N_2O flush following N fertilization. They were done as follows: 1 day before fertilization, 3, 5 and 7 days after fertilization, once a week in the 4 weeks that followed fertilization and twice a month in the second to the sixth month after fertilization. The obtained gas samples were stored in pre-evacuated airtight 12 mL Labco exetainers® fitted with Labco Grey Chlorobutyl Septum and quarter-turned plastic screw caps (Labco Ltd, Lampeter, UK) which minimized gas leakages during storage and transportation. The gas-filled exetainers were periodically transferred (within a maximum of 120 days from sampling) to a laboratory at ETH Zürich, Switzerland, where GHG concentrations in the obtained gas samples were analysed with gas chromatography (GC; Scion 456-GC Bruker, Germany). A total of 1200 pooled gas samples were obtained over the sampling period (14 months). Soil N_2O fluxes were calculated based on the Hüppi et al. (2018) scheme implemented using the online Soil GHG flux shiny tool.

2.5 | Productivity and profitability

With respect to productivity, we harvested four random 1 m × 1 m quadrants in every treatment plot of the CRD experiment at about 16 months (green circles; Figure 1b) and weighed the field fresh weight from every quadrant to determine biomass. Note that our field fresh weight data only represents biomass/yield estimates from sugarcane fields with minimal sprouting failures. Next, we determined crop N uptake by multiplying the mean dry biomass by its N content determined from the C/N Analyser (Vario EL cube; Elementar Analysis Systems GmbH, Hanau, Germany) at the University of Augsburg, Germany. Partial factor productivity—an integrative index that quantifies the total economic output of the respective fertilization regimes relative to the utilization of the applied N (Antille & Moody, 2021) was estimated by dividing the field fresh weight from the respective CRD treatment plots by their corresponding N fertilizer rates. Return on investment was determined by obtaining data on the factory price of sugarcane field fresh weight (80,000–280,000 Ugandan shillings, UGX) and the market price of urea fertilizers for the years 2018 through 2022 (about 106,000 UGX) from Masindi Sugarcane Growers' Association. We converted the local prices to US dollars using the average world bank exchange rate for the period 2018–2022. Next, using field fresh weight estimates for the production cycle 2019–2020 and maintaining the same N application rates (low, standard and high) across 2018 and 2022, we determined how fluctuating market prices

of fertilizers and fairly constant prices of sugarcane biomass as per the account of the focal point person (Chairperson) at Masindi Sugarcane Grower's Association affected the return on investment under different fertilization regimes over a 5 year period (2018–2022).

2.6 | Statistical analyses

Differences in soil N leaching flux, plant N uptake, soil N_2O emissions, field fresh weight and partial factor productivity among the CRD treatments were analysed using univariate analysis of variance (ANOVA) followed by the post hoc Tukey's honestly significant difference (HSD) test for multiple comparison between treatment groups. Before running the ANOVA, we checked whether all the response variables were normally distributed based on quantile–quantile (QQ) plots and Shapiro tests and if their respective variances were homogeneous based on the Levene test. Except for the soil N_2O fluxes, all the other response variable datasets, namely, soil N leaching flux, plant N uptake, field fresh weight and partial factor productivity, were Tukey transformed before running the ANOVA analyses because they showed a non-normal distribution and heteroscedasticity. All the statistical analyses were done in R 3.6.3 (R Development Core Team, 2022) using the 'rcompanion' package for the normality and homoscedasticity check as well as the Tukey transformation and the 'car' package for the univariate ANOVA and posthoc Tukey's HSD tests. For all the analyses, statistical significance was inferred at p value < 0.05.

3 | RESULTS

3.1 | Estimation of drainage fluxes and soil water balance components

All the five PTFs predicted soil hydraulic parameters that ranged between 0 and 0.108 $cm^3 cm^{-3}$ for θ_r, 0.450 and 0.555 $cm^3 cm^{-3}$ for θ_s, 0.011 and 0.630 cm^{-1} for α, 1.079 and 1.419 for n (Table 2). Regarding the hydraulic conductivity function, all five PTFs predicted K_s values ranging between 6 and 109 $cm\,d^{-1}$ for the topsoil layer (0–10 cm) and between 3 and 155 $cm\,d^{-1}$ for the subsurface layers (10–100 cm; Table 2).

Evaluation of the performance of the five PTFs was based on the comparison between simulated and measured soil matric potential values at $z = 60$ cm and $z = 90$ cm (Figure 3). RAWLS82, ROSETTA and WOS99 PTFs estimated soil matric potentials that closely matched the measured matric potentials (Figure 3a–d, i–j; Figure A4) on the premise of the lowest RMSEs (58–121 cm; Figure 3a–d, i–j) and the highest R^2 (0.44–0.91; Figure 3a–d, i–j) and d (0.67–0.89; Figure 3a–d, i–j) indices. In addition, their NSE values ranged between 0 and 1 at the soil depth of 60 cm and between −0.71 and 0 at the soil depth of 90 cm (Figure 3a–d, i–j). On the contrary, soil matric potential estimated by T&H98 and WEY09 PTFs poorly matched observed matric potential values. As a result, these PTFs (T&H98 and WEY09) obtained the lowest performance indicated by high RMSEs (127–309 cm), low R^2 (0.12–0.82) and d (0.22–0.79) (Figure 3e–h) and more negative NSE values in comparison to RAWLS82, ROSETTA and WOS99 PTFs (Figure 3a–d, i–j). Given the above-mentioned performance metrics, we derived the mean annual water balance components (runoff, drainage, evaporation, transpiration and storage; Table 3; Figure A3) based on RAWLS82, ROSETTA and WOS99 PTFs. Accordingly, we estimated that on average, drainage, surface evaporation and transpiration represented 41%, 24% and 35% respectively, of the annual precipitation (1716 mm) while runoff and deep storage—annual net change in the profile of soil water content were negligible (0%–0.7%; Table 3).

3.2 | Nitrogen leaching flux and soil nitrous oxide emissions

N leaching fluxes estimated by multiplying soil water drainage fluxes from the water subroutine of LEACHM and the measured soil solution N concentration from the suction cup lysimeters show that addition of N fertilizers at different rates (low, standard and high) resulted in varying N leaching fluxes across space (Figure 4a) and time (Figure 5a).

Mean annual N leaching flux measured from the low (1.7 ± 0.6 $kg\,N\,ha^{-1}\,year^{-1}$; Figure 4a) and standard N (3.4 ± 0.7 $kg\,N\,ha^{-1}\,year^{-1}$; Figure 4a) treatment plots were comparable ($p = 0.150$) but both significantly lower than the mean annual N leaching flux measured from high N treatment plots (14.2 ± 2.2 $kg\,N\,ha^{-1}\,year^{-1}$; $Df = 2$; F-value = 25.7; $p < 0.001$; Figure 4a). N leaching fluxes at 90 cm in all treatments peaked around the third and eighth week following fertilization (Figure 5a), periods that corresponded to the largest rainfall amounts following fertilization (Figure 5b). The N leaching fluxes thereafter declined to the background levels (Figure 5a) for the rest of the sampling period in all treatment plots except in the high fertilization treatment plots where relatively weak N leaching pulses were observed in the 17th and 21st weeks (Figure 5a). Notably, urea fertilization did not alter the magnitude of soil N_2O emissions along the fertilizer intensification gradient (~0.2 to 0.3 $kg\,N\,ha^{-1}\,year^{-1}$; $Df = 2$; F-value = 0.164; $p = 0.851$; Figure 4b).

TABLE 2 The residual water content (θ_r), saturated water content (θ_s), soil water retention function shape parameters (α and n) and saturated hydraulic conductivity (K_s) at the soil depths of 0–10, 10–30, 30–50 and 50–100 cm estimated by five pedotransfer functions (PTFs; RAWLS82, ROSETTA, T&H98, WEY09 and WOS99).

PTF	Soil hydraulic parameters	Soil depth (cm)			
		0–10	10–30	30–50	50–100
RAWLS82	θ_r ($cm^3 cm^{-3}$)	0	0	0	0
	θ_s ($cm^3 cm^{-3}$)	0.459	0.461	0.515	0.538
	α (cm^{-1})	0.060	0.067	0.022	0.016
	n (–)	1.157	1.129	1.100	1.105
	K_s (cm d^{-1})	81.0	100.0	11.7	6.7
ROSETTA	θ_r ($cm^3 cm^{-3}$)	0.081	0.088	0.106	0.108
	θ_s ($cm^3 cm^{-3}$)	0.519	0.491	0.530	0.552
	α (cm^{-1})	0.017	0.019	0.024	0.024
	n (–)	1.419	1.376	1.282	1.281
	K_s (cm d^{-1})	69.7	34.8	32.3	38.6
T&H98	θ_r ($cm^3 cm^{-3}$)	0	0	0	0
	θ_s ($cm^3 cm^{-3}$)	0.515	0.501	0.503	0.512
	α (cm^{-1})	0.397	0.448	0.630	0.450
	n (–)	1.160	1.138	1.096	1.093
	K_s (cm d^{-1})	101	112	155	111
WEY09	θ_r ($cm^3 cm^{-3}$)	0	0	0	0
	θ_s ($cm^3 cm^{-3}$)	0.494	0.478	0.509	0.521
	α (cm^{-1})	0.016	0.015	0.011	0.011
	n (–)	1.167	1.134	1.083	1.079
	K_s (cm d^{-1})	6.17	5.12	3.07	2.99
WOS99	θ_r ($cm^3 cm^{-3}$)	0	0	0	0
	θ_s ($cm^3 cm^{-3}$)	0.528	0.487	0.517	0.545
	α (cm^{-1})	0.047	0.052	0.023	0.015
	n (–)	1.157	1.109	1.099	1.114
	K_s (cm d^{-1})	109	20	11	13

3.3 | Productivity and profitability of sugarcane cultivation at increasing N rates

Mean field fresh weight ranged between 124±12 and 192±27 Mg FFW $ha^{-1} year^{-1}$ (Figure 6a), however, there was no significant differences between treatments ($Df=2$; F-value = 3.051; $p=0.057$; Figure 6a). Similarly, mean N uptake ranged between 61.9±5.8 and 93.5±13.6 kg N $ha^{-1} year^{-1}$ but no significant differences were detected between treatments ($Df=2$; F-value = 1.972; $p=0.151$; Figure 6b). With respect to partial factor productivity, utilization of the applied fertilizer was significantly higher at low N fertilization rates (3.5±0.4 Mg FFW ha^{-1} kg N ha^{-1}) in comparison to both the standard (2.4±0.2 Mg FFW ha^{-1} kg N ha^{-1}) and higher N fertilization rates (1.8±0.3 Mg FFW ha^{-1} kg N ha^{-1}; $Df=2$; F-value = 10.9; $p<0.001$; Figure 6c).

Contrary to the no significant increment in field fresh weight along the fertilizer intensification gradient (low < standard < high; Figure 6a), return on investment declined by ~31% (from 114 to 79 USD FFW USD^{-1} N fertilizer) when N fertilization rates were increased from low to standard and by ~25% (from 79 to 59 USD FFW USD^{-1} N fertilizer) when N fertilization rates exceeded the standard, in the base year (2018) and so did in years, 2019 and 2020 (Figure 6d). However, in the period between 2021 and 2022, when the market price of fertilizer increased nearly fourfold against the inelastic factory price for field fresh weight compared to the base year (2018), return on investment declined by almost 65% across all treatments (Figure 6d).

4 | DISCUSSION

4.1 | PTF performance for estimating the hydraulic properties of Ferralsols

The N leaching part of the study was based on the simulation of water flux in the soil–plant-atmosphere continuum in LEACHM. However, knowledge of the soil water retention and hydraulic conductivity functions was needed as it represents a fundamental prerequisite for

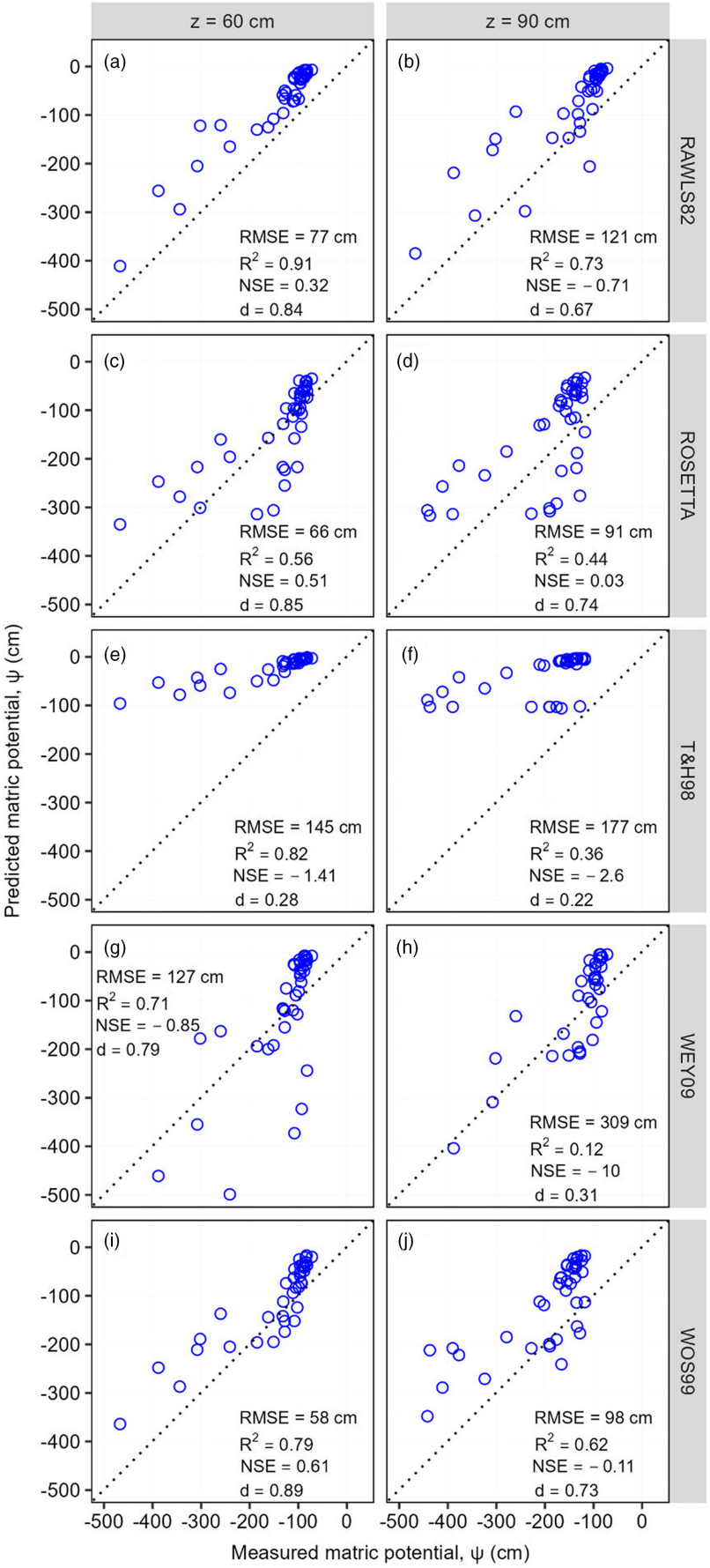

FIGURE 3 Predicted and measured soil matric potential based on RAWLS82 (a, b), ROSETTA (c, d), T&H98 (e, f), WEY09 (g, h) and WOS99 (i, j) pedotransfer functions at soil depths of 60 and 90 cm. The corresponding root mean square error (RMSE), coefficient of determination (R^2), Nash Sutcliffe efficiency (NSE) and the index of agreement (d) are reported in each subplot.

TABLE 3 Annual soil water balance components (runoff, drainage, evaporation, transpiration and storage) derived from annual precipitation (1716 mm) using the three best performing PTFs; RAWLS82, ROSETTA and WOS99.

PTF	Runoff (mm)	Drainage (mm)	Evaporation (mm)	Transpiration (mm)	Storage (mm)
RAWLS82	0	735	365	595	20
ROSETTA	0	713	407	595	0
WOS99	0	739	367	595	15
Mean (±standard error, SE; $N=3$)	0 ± 0	729 ± 8	380 ± 14	595 ± 0	12 ± 6

reliable simulations of drainage fluxes (Dane & Clarke Topp, 2002). Direct measurements of soil hydraulic properties entail large-scale field campaigns to collect soil samples and laboratory experiments, which are often tedious, labour-intensive and time-consuming (Gijsman et al., 2002; Nasta et al., 2021) and hard to implement and maintain in remote rural regions of SSA. Hence, under these circumstances, we opted to estimate the soil hydraulic parameters from readily available soil physical data using well-established PTFs (Van Looy et al., 2017).

We had postulated in the first hypothesis that the Brazilian PTF would be an optimal predictor of soil hydraulic properties at our study site in tropical Africa compared to its temperate counterparts. However, we were surprised to find that RAWLS82, ROSETTA and WOS99 PTFs trained in the northern hemisphere under temperate climate conditions led to satisfactory model performance based on the comparison between simulated and observed soil matric potential values at soil depths of 60 and 90 cm (Figure 3a–d, i–j) while T&H98 and WEY09 PTFs obtained the lowest performance (Figure 3e–h). Thus our hypothesis that PTFs trained in tropical environments outcompete their temperate counterparts was rejected. We argue that the good performance of RAWLS82, ROSETTA and WOS99 is related to the broad variety of soil physico-chemical settings that they have been tested and calibrated on, hence these PTFs are sensitive to a broad spectrum of soil bulk densities. T&H98 (from the tropics) and WEY09 (temperate regions) PTFs, were less suited for our test site in SSA in predicting the soil hydraulic properties because these two PTFs are relatively site specific and do not exploit bulk density in the estimation of soil water retention and hydraulic conductivity function (Table A1). Yet, soil bulk density is a proxy for soil structure and exerts a direct control on soil porosity and soil permeability. Hence, ignoring soil bulk density in the estimation of hydraulic properties compromises the performance of the PTF and limits its application to sites with bulk density similar to the original test and calibration sites. Consequently, these two PTFs (T&H98 and WEY09) had the biggest RMSE values at the two evaluated depths (Figure 3e–h) compared to their counterparts (RAWLS82, ROSETTA and WOS99; Figure 3a–d, i–j). In light of the observed differences in the PTF performance at our tropical test site, our study findings highlight that future studies always need to validate PTF estimates of soil hydraulic properties with in-situ measurements of either matric potential or soil water content.

4.2 | Treatment effects on nitrogen losses

Contrary to the second hypothesis, soil N_2O emissions (Figure 4b) were very low across all the treatments and so were the N leaching losses except at the higher-than-standard N rate where we measured high N leaching losses (Figure 4a). Furthermore, these findings contrast the wider recognition that increased N availability not only amplifies soil N_2O emissions through elevated nitrification and denitrification processes (Friedl et al., 2023; Takeda et al., 2021, 2022) but also increases N loads in groundwater aquifers below fertilizer-based agro-catchments (Huang et al., 2017; Russo et al., 2017). For this study, we postulate that the low soil N_2O emissions (Figure 4b) and N leaching losses particularly in low and standard treatments (Figure 4a) were the result of N fertilization closely matching the sugarcane crop N demands thus riding the respective systems of excess nitrogen which would have led to increased soil N_2O emisisions and N leaching losses. Armour et al. (2013) and Ghiberto et al. (2011) similarly found low N leaching losses under variably fertilized Brazilian and Australian sugarcane plantations, respectively, and attributed the meagre N leaching losses to the high N demand by the sugarcane crop.

4.3 | Treatment effects on the productivity and profitability of sugarcane

4.3.1 | Biomass productivity

Consistent with the third hypothesis, we measured an increase in field fresh weight at increasing N fertilizer rates because N availability has been shown to stimulate photosynthetic traits of sugarcane especially the chlorophyll content, stomatal conductance, leaf area, specific leaf nitrogen content, photosynthetic rate, plant height and total leaves

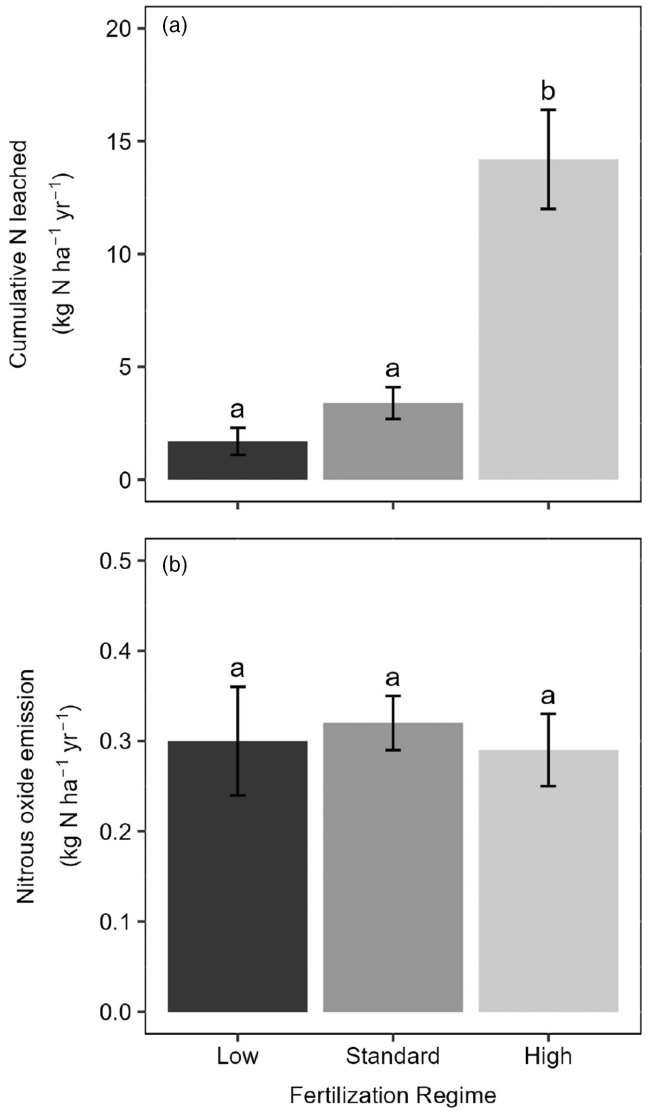

FIGURE 4 Mean (±standard error, SE) annual N leached (a) and nitrous oxide emissions (b) under low, standard and high fertilization regimes. The value of N leached (panel a) are mean N concentrations in the leachate obtained from two suction cup lysimeters installed in three of the four plots for low, standard and high treatments ($n = 3$) and mean drainage fluxes based on three best performing pedotransfer functions (RAWLS82, ROSETTA and WOS99) while the values of nitrous oxide emissions in panel (b) are means of four plots ($n = 4$). Lowercase letters in panels (a) and (b) indicate significant differences between treatments (ANOVA with Tukey's HSD test with a multiple-comparison extension test at $p \leq 0.05$).

(Dinh et al., 2017; Lofton & Tubaña, 2015) as well as increase the millable cane length, girth and weight (Tayade et al., 2020). It is, however, surprising that the measured increase in field fresh weight did not translate to significant differences among treatments (Figure 6a). The reasons for this finding are unclear, but may be related to sugarcane meeting its N requirements through the mineralization of soil organic matter at the study site as similarly reported by Otto et al. (2016). Otto et al. (2016) found none to moderate responsiveness of sugarcane field fresh weight to N fertilization in nearly 34 of the 45 established experimental trials in Brazil and attributed this to the sufficient supply of N from the mineralization of the soil organic matter stocks. Additionally, we suspect that despite randomizing the biomass measurements in every treatment plot, we may have inadvertently underrepresented sprouting failures in our biomass measurements resulting in high variability of the biomass estimates. Stubble bud sprouting failures in ratoon cane fields (due to pests, diseases and mechanical damage) have been shown to result in low shoot populations and reduced cane yields (Jain et al., 2007; Shukla et al., 2009). Notwithstanding, our field fresh weight estimates across all the treatments (low, standard and high; 124–192 Mg ha^{-1}) were comparable (~180 Mg ha^{-1}) to those reported by Tayade et al. (2020) but higher than those (30–150 Mg ha^{-1}) reported by Lofton and Tubaña (2015), Premalatha et al. (2016) and Yadav (2004). We think that the differences in sugarcane biomass observed among studies reflect the differences in climatic conditions and N application rates used in the respective experimental setups.

4.3.2 | Partial factor productivity and profitability

Our analyses of partial factor productivity under the different fertilizer regimes revealed a decline in the estimated partial factor productivity at increasing fertilizer application rates (Figure 6c) contravening the third hypothesis. The declining partial factor productivity at increasing N rates reflects better utilization of the applied N fertilizer at lower N doses compared to higher N doses due to the much higher physiological efficiency of the sugarcane crop under N-limited conditions. The findings on partial factor productivity are comparable to those reported by Premalatha et al. (2016) in Indian sugarcane fields and Thorburn et al. (2017, 2013) in Australian sugarcane fields but are on the upper end of the worldwide partial factor productivity ranges for sugarcane (0.25–0.9 Mg FFW kg^{-1} N; Thorburn et al., 2013) mainly because partial factor productivity was a derivative of the much higher field fresh weight. Similarly, the measured decline in return on investment at increasing N rates (Figure 6d) further reinforces our basis for rejecting the third hypothesis in which we had postulated that higher N rates would be more profitable than low N rates. Hence, on the basis of these findings, the low N rates seem promising due to a higher partial factory productivity and return on investment and comparable field fresh weight, soil N_2O emissions and N leaching losses to the standard N rate. Nonetheless, it is worth highlighting that profitability of the different

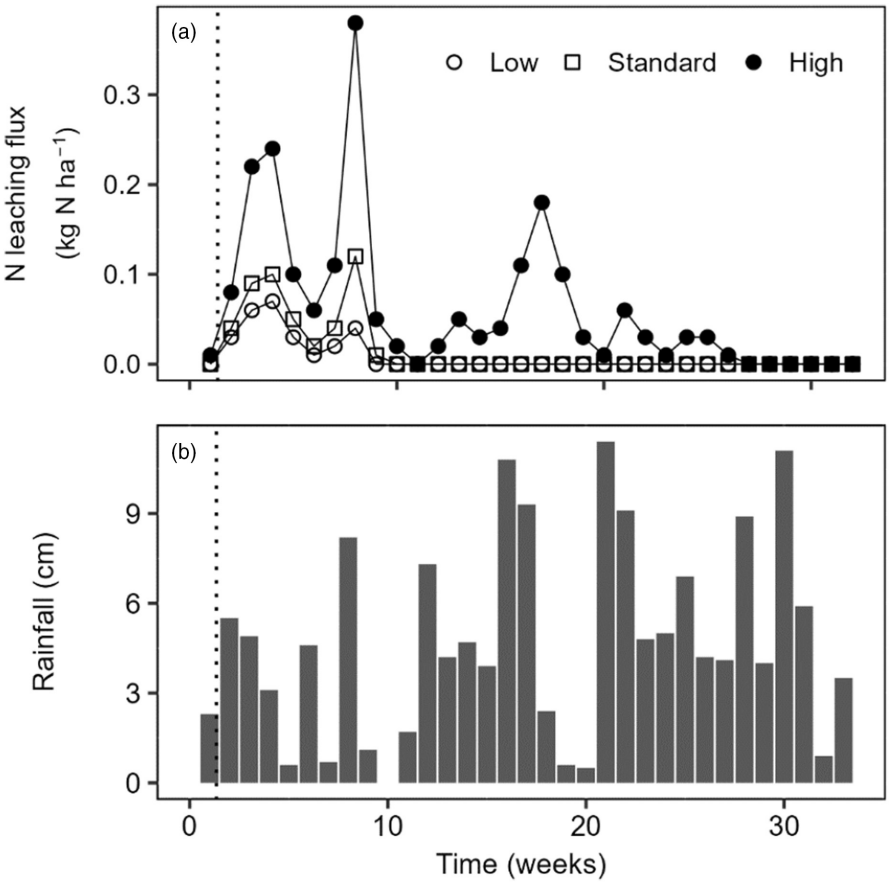

FIGURE 5 (a) Mean weekly *N* leaching flux from low, standard and high fertilization regimes and (b) weekly rainfall sums between April and December 2019. The vertical dotted line in panels (a) and (b) indicates the timing of a single-dose fertilizer application in the treatment plots.

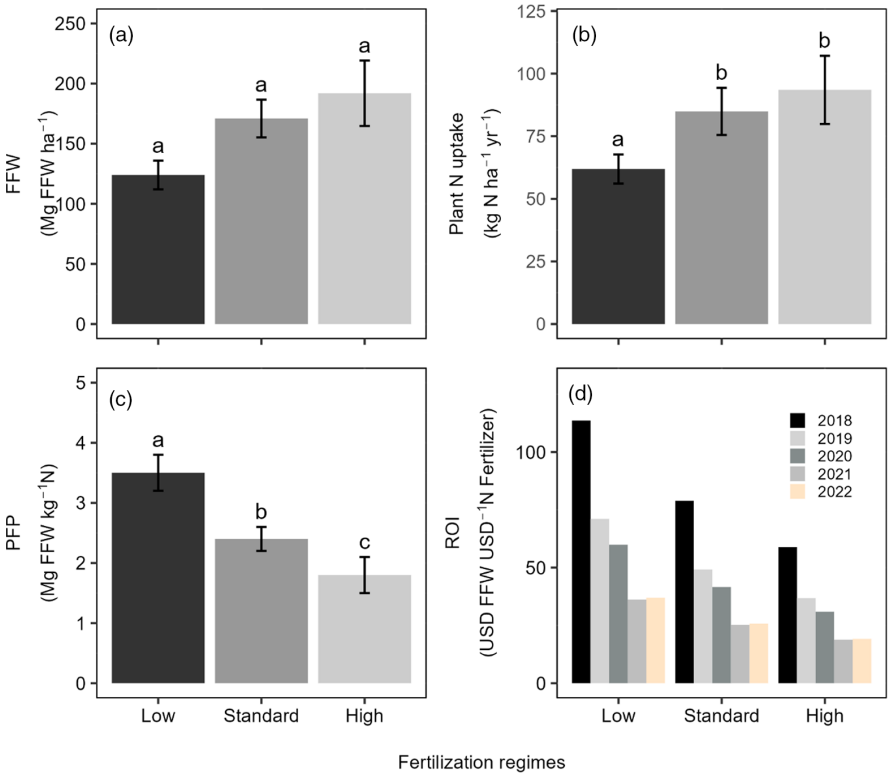

FIGURE 6 Mean (±standard error, SE, $n = 4$) field fresh weight (FFW; a), plant N uptake (b), partial factor productivity (PFP; c) and return on investment (ROI; d) along the fertilizer intensification gradient (low, standard and high). Lowercase letters in panels (a), (b) and (c) indicate significant differences between treatments (ANOVA with Tukey's HSD test with a multiple-comparison extension test at $p \leq 0.05$).

regimes is largely dependent on the stability of the factory and market prices of sugarcane biomass and fertilizers, respectively, since our analyses demonstrated that in the years when the market price of fertilizers increased four-fold against a stagnant factory price of field fresh weight, application of fertilizers, even at the lowest N rate equally

resulted a significant shrinkage of the return on investment margins (Figure 6d).

5 | CONCLUSION

Our study provides new insights into nitrogen management in fertilizer-intensive sugarcane plantations in sub-Saharan Africa. Using a detailed completely randomized experiment with three levels of nitrogen fertilization, we decipher the link between nitrogen levels, environmental impacts and agricultural outcomes. Our results not only show the effectiveness of some pedotransfer functions in predicting nitrogen leaching losses, especially in data-poor areas of sub-Saharan Africa but also highlight how any increases above the standard nitrogen fertilization rate for sugarcane ratoon crops lead to significant increases in nitrogen leaching losses in these systems. Similarly, although we detected no significant differences in the measured soil nitrous oxide emissions and field fresh weight, the decline in partial factor productivity and return of investment along the fertilizer intensification gradient shows possible trade-offs if higher levels of nitrogen are used. Collectively, the study findings suggest that the observed robustness of some pedotransfer functions along with the possibility of achieving comparable sugarcane yields at lower-than-standard nitrogen fertilization rates creates a viable opportunity to address groundwater pollution and greenhouse gas emissions challenges in sub-Saharan African sugarcane plantations. However, there is a need for more studies focusing on nitrogen fertilization optimization strategies and the long-term impacts of different fertilizer management on soil quality and sugarcane yields in the sub-Saharan African region.

ACKNOWLEDGEMENTS

This study was funded by the German Academic Exchange (DAAD, Germany, grant number: 57381412, 2018), the National Agricultural Research Organization (NARO, Uganda), the International Foundation for Science (IFS, Sweden, grant number: D/6293–1, 2019) and the German Research Foundation (DFG, Germany) funded Emmy Noether Junior Research Group 'TropSOC' (Gepris—project number 387472333, 2017). We would like to thank management of the Sustainable Agroecosystems' and Soil resources' laboratories ETH Zürich, for analysing all the gas samples. The authors are also grateful to the management of Walji Sugarcane Estate, Kanyege, Masindi district, Uganda, for hosting the experiment, as well as G.B. Ayo and M. Adriko for supporting our field activities. Open Access funding enabled and organized by Projekt DEAL.

CONFLICT OF INTEREST STATEMENT

The authors declare that there are no conflicts of interest.

DATA AVAILABILITY STATEMENT

All the data supporting the findings of this study are accessible at https://doi.org/10.5281/zenodo.8284582.

ORCID

Peter Fiener https://orcid.org/0000-0001-6244-4705

REFERENCES

Aina, P. O., & Periaswamy, S. P. (1985). Estimating available water-holding capacity of western Nigerian soils from soil texture and bulk density, using core and sieved samples. *Soil Science*, *140*, 55–58. https://doi.org/10.1097/00010694-198507000-00007

Allen, D. E., Kingston, G., Rennenberg, H., Dalal, R. C., & Schmidt, S. (2010). Effect of nitrogen fertilizer management and waterlogging on nitrous oxide emission from subtropical sugarcane soils. *Agriculture, Ecosystems & Environment*, *136*, 209–217. https://doi.org/10.1016/j.agee.2009.11.002

Allen, G. R., Pereira, S. L., Raes, D., & Smith, M. (1998). *Crop evapotranspiration-guidelines for computing crop water requirements-FAO irrigation and drainage paper 56*. Food and Agriculture Organization.

Antille, D. L., & Moody, P. W. (2021). Nitrogen use efficiency indicators for the Australian cotton, grains, sugar, dairy and horticulture industries. *Environmental and Sustainability Indicators*, *10*, 1–10. https://doi.org/10.1016/j.indic.2020.100099

Arias-Navarro, C., Díaz-Pinés, E., Kiese, R., Rosenstock, T. S., Rufino, M. C., Stern, D., Neufeldt, H., Verchot, L. V., & Butterbach-Bahl, K. (2013). Gas pooling: A sampling technique to overcome spatial heterogeneity of soil carbon dioxide and nitrous oxide fluxes. *Soil Biology and Biochemistry*, *67*, 20–23. https://doi.org/10.1016/j.soilbio.2013.08.011

Armour, J. D., Nelson, P. N., Daniells, J. W., Rasiah, V., & Inman-Bamber, N. G. (2013). Nitrogen leaching from the root zone of sugarcane and bananas in the humid tropics of Australia. *Agriculture, Ecosystems & Environment*, *180*, 68–78. https://doi.org/10.1016/j.agee.2012.05.007

Batsukh, K., Zlotnik, V. A., Suyker, A., & Nasta, P. (2021). Prediction of biome-specific potential evapotranspiration in Mongolia under a scarcity of weather data. *Water*, *13*, 1–20. https://doi.org/10.3390/w13182470

Bijay-Singh, & Craswell, E. (2021). Fertilizers and nitrate pollution of surface and groundwater: An increasingly pervasive global problem. *SN Applied Sciences*, *3*, 1–24. https://doi.org/10.1007/s42452-021-04521-8

Blum, J., Melfi, A. J., Montes, C. R., & Gomes, T. M. (2013). Nitrogen and phosphorus leaching in a tropical Brazilian soil cropped with sugarcane and irrigated with treated sewage effluent. *Agricultural Water Management*, *117*, 115–122. https://doi.org/10.1016/j.agwat.2012.11.010

Bordonal, R. d. O., Carvalho, J. L. N., Lal, R., de Figueiredo, E. B., de Oliveira, B. G., & La Scala, N. (2018). Sustainability of sugarcane production in Brazil. A review. *Agronomy for Sustainable Development*, *38*, 1–23. https://doi.org/10.1007/s13593-018-0490-x

Brumbley, S. M., Snyman, S. J., Gnanasambandam, A., Joyce, P., Hermann, S. R., da Silva, J. A. G., McQualter, R. B., Wang, M.-L., Egan, B. T., Paterson, A. H., Albert, H. H., & Moore, P. H.

(2008). Sugarcane. In C. Kole & T. C. Hall (Eds.), *Compendium of transgenic crop plants* (pp. 1–58). John Wiley & Sons, Ltd. https://doi.org/10.1002/9781405181099.k0701

Carmo, J. B. d., Filoso, S., Zotelli, L. C., de Sousa Neto, E. R., Pitombo, L. M., Duarte-Neto, P. J., Vargas, V. P., Andrade, C. A., Gava, G. J. C., Rossetto, R., Cantarella, H., Neto, A. E., & Martinelli, L. A. (2013). Infield greenhouse gas emissions from sugarcane soils in Brazil: Effects from synthetic and organic fertilizer application and crop trash accumulation. *Global Change Biology. Bioenergy*, *5*, 267–280. https://doi.org/10.1111/j.1757-1707.2012.01199.x

Cherubin, M. R., Franco, A. L. C., Cerri, C. E. P., da Oliveira, D. M. S., Davies, C. A., & Cerri, C. C. (2015). Sugarcane expansion in Brazilian tropical soils—Effects of land use change on soil chemical attributes. *Agriculture, Ecosystems & Environment*, *211*, 173–184. https://doi.org/10.1016/j.agee.2015.06.006

Conlong, D. E., & Mugalula, A. (2001). Eldana saccharina (Lep: Pyralidae) andits parasitoids at Kinyara sugar works, Uganda. *Proceedings of the South African Sugar Technologists' Association*, *75*, 183–185.

da Silva, A. C., Armindo, R. A., Brito, A. d. S., & Schaap, M. G. (2017). An assessment of pedotransfer function performance for the estimation of spatial variability of key soil hydraulic properties. *Vadose Zone Journal*, *16*, 1–10. https://doi.org/10.2136/vzj2016.12.0139

Dane, J. H., & Clarke Topp, G. (2002). *Methods of soil analysis: Part 4 physical methods, SSSA book series*. Soil Science Society of America. https://doi.org/10.2136/sssabookser5.4

Dattamudi, S., Wang, J. J., Dodla, S. K., Viator, H. P., DeLaune, R., Hiscox, A., Darapuneni, M., Jeong, C., & Colyer, P. (2019). Greenhouse gas emissions as influenced by nitrogen fertilization and harvest residue management in sugarcane production. *Agrosystems, Geosciences & Environment*, *2*, 1–10. https://doi.org/10.2134/age2019.03.0014

de Morais, L. K., de Aguiar, M. S., de Albuquerque e Silva, P., Câmara, T. M. M., Cursi, D. E., Júnior, A. R. F., Chapola, R. G., Carneiro, M. S., & Bespalhok Filho, J. C. (2015). Breeding of sugarcane. In V. M. V. Cruz & D. A. Dierig (Eds.), *Industrial Crops* (pp. 29–42). Handbook of Plant Breeding. Springer New York. https://doi.org/10.1007/978-1-4939-1447-0_2

Dinh, T. H., Watanabe, K., Takaragawa, H., Nakabaru, M., & Kawamitsu, Y. (2017). Photosynthetic response and nitrogen use efficiency of sugarcane under drought stress conditions with different nitrogen application levels. *Plant Production Science*, *20*, 412–422. https://doi.org/10.1080/1343943X.2017.1371570

Forster, P., Ramaswamy, V., Artaxo, P., Berntsen, T., Betts, R., Fahey, D. W., Haywood, J., Lean, J., Lowe, D. C., Myhre, G., Nganga, J., Prinn, R., Raga, G., Schulz, M., & Van Dorland, R. (2007). Changes in atmospheric constituents and in radiative forcing. In S. Solomon, D. Qin, M. Manning, Z. Chen, M. Marquis, K. B. Averyt, M. Tignor, & H. L. Miller (Eds.), *Climate change 2007: The physical science basis. Contribution of working group I to the fourth assessment report of the intergovernmental panel on climate change*. Cambridge University Press.

Franco, H. C. J., Otto, R., Faroni, C. E., Vitti, A. C., Almeida de Oliveira, E. C., & Trivelin, P. C. O. (2011). Nitrogen in sugarcane derived from fertilizer under Brazilian field conditions. *Field Crops Research*, *121*, 29–41. https://doi.org/10.1016/j.fcr.2010.11.011

Friedl, J., Warner, D., Wang, W., Rowlings, D. W., Grace, P. R., & Scheer, C. (2023). Strategies for mitigating N_2O and N_2 emissions from an intensive sugarcane cropping system. *Nutrient Cycling in Agroecosystems*, *125*, 295–308. https://doi.org/10.1007/s10705-023-10262-4

Furtado da Silva, N., Cabral da Silva, E., Muraoka, T., Batista Teixeira, M., Antonio Loureiro Soares, F., Nobre Cunha, F., Adu-Gyamfi, J., & Cavalcante, W. S. d. S. (2020). Nitrogen utilization from ammonium nitrate and urea fertilizer by irrigated sugarcane in Brazilian Cerrado Oxisol. *Agriculture*, *10*, 1–17. https://doi.org/10.3390/agriculture10080323

Gee, G. W., & Or, D. (2002). 2.4 particle-size analysis. In J. H. Dane & G. Clarke Topp (Eds.), *SSSA Book Series* (pp. 255–293). Soil Science Society of America. https://doi.org/10.2136/sssabookser5.4.c12

Ghiberto, P. J., Libardi, P. L., Brito, A. d. S., & Trivelin, P. C. O. (2011). Nitrogen fertilizer leaching in an Oxisol cultivated with sugarcane. *Scientia Agricola (Piracicaba, Braz.)*, *68*, 86–93. https://doi.org/10.1590/S0103-90162011000100013

Ghiberto, P. J., Libardi, P. L., Brito, A. S., & Trivelin, P. C. O. (2009). Leaching of nutrients from a sugarcane crop growing on an Ultisol in Brazil. *Agricultural Water Management*, *96*, 1443–1448. https://doi.org/10.1016/j.agwat.2009.04.020

Gijsman, A. J., Jagtap, S. S., & Jones, J. W. (2002). Wading through a swamp of complete confusion: How to choose a method for estimating soil water retention parameters for crop models. *European Journal of Agronomy*, *18*, 77–106. https://doi.org/10.1016/S1161-0301(02)00098-9

Guarracino, L. (2007). Estimation of saturated hydraulic conductivity Ks from the van Genuchten shape parameter α. *Water resources research*, *43*, 1–4. https://doi.org/10.1029/2006WR005766

Holzworth, D. P., Huth, N. I., de Voil, P. G., Zurcher, E. J., Herrmann, N. I., McLean, G., Chenu, K., van Oosterom, E. J., Snow, V., Murphy, C., Moore, A. D., Brown, H., Whish, J. P. M., Verrall, S., Fainges, J., Bell, L. W., Peake, A. S., Poulton, P. L., Hochman, Z., … Keating, B. A. (2014). APSIM—Evolution towards a new generation of agricultural systems simulation. *Environmental Modelling & Software*, *62*, 327–350. https://doi.org/10.1016/j.envsoft.2014.07.009

Huang, T., Ju, X., & Yang, H. (2017). Nitrate leaching in a winter wheat-summer maize rotation on a calcareous soil as affected by nitrogen and straw management. *Scientific Reports*, *7*, 42247. https://doi.org/10.1038/srep42247

Hüppi, R., Felber, R., Krauss, M., Six, J., Leifeld, J., & Fuß, R. (2018). Restricting the nonlinearity parameter in soil greenhouse gas flux calculation for more reliable flux estimates. *PLoS ONE*, *13*, 1–17. https://doi.org/10.1371/journal.pone.0200876

Hutson, J. L. (2003). LEACHM—a process-based model of water and solute movement, transformations, plant uptake and chemical reactions in the unsaturated zone, version 4. Department of Crop and Soil Sciences, research series No. R03-1, Cornell University, Ithaca, New York.

IUSS Working Group WRB. (2015). World Reference Base for soil resources 2014, update 2015 international soil classification system for naming soils and creating legends for soil maps. (World Soil Resources Reports No. 106). FAO, Rome.

Jain, R., Shrivastava, A. K., Solomon, S., & Yadav, R. L. (2007). Low temperature stress-induced biochemical changes affect stubble bud sprouting in sugarcane (Saccharum spp. hybrid). *Plant*

Growth Regulation, *53*, 17–23. https://doi.org/10.1007/s10725-007-9199-6

Ju, X., & Zhang, C. (2017). Nitrogen cycling and environmental impacts in upland agricultural soils in North China: A review. *Journal of Integrative Agriculture*, *16*, 2848–2862. https://doi.org/10.1016/S2095-3119(17)61743-X

Leff, B., Ramankutty, N., & Foley, J. A. (2004). Geographic distribution of major crops across the world. *Global Biogeochemical Cycles*, *18*, 1–33. https://doi.org/10.1029/2003GB002108

Lehto, T., Westerhof, A. B., Lehtonen, M. I., Manninen, T., Mäkitie, H., Virransalo, P., Pokki, J., Härmä, P., Koistinen, T., Saalmann, K., Kuosmanen, E., Mänttäri, I., Katto, E., Baguma, Z., de Kock, G., & Elepu, D. (2014). Geological map of Uganda.

Lofton, J., & Tubaña, B. (2015). Effect of nitrogen rates and application time on sugarcane yield and quality. *Journal of Plant Nutrition*, *38*, 161–176. https://doi.org/10.1080/01904167.2013.828752

Lukwago, W., Behangana, M., Mwavu, E. N., & Hughes, D. F. (2020). Effects of selective timber harvest on amphibian species diversity in Budongo forest reserve, Uganda. *Forest Ecology and Management*, *458*, 1–7. https://doi.org/10.1016/j.foreco.2019.117809

Meier, E. A., Thorburn, P. J., Wegener, M. K., & Basford, K. E. (2006). The availability of nitrogen from sugarcane trash on contrasting soils in the wet tropics of North Queensland. *Nutrient Cycling in Agroecosystems*, *75*, 101–114. https://doi.org/10.1007/s10705-006-9015-0

Mello, F. F. C., Cerri, C. E. P., Davies, C. A., Holbrook, N. M., Paustian, K., Maia, S. M. F., Galdos, M. V., Bernoux, M., & Cerri, C. C. (2014). Payback time for soil carbon and sugar-cane ethanol. *Nature Climate Change*, *4*, 605–609. https://doi.org/10.1038/nclimate2239

Meyer, J. H., & Antwerpen, R. v. (2010). Advances in sugarcane soil fertility research in southern Africa. *South African Journal of Plant and Soil*, *27*, 19–31. https://doi.org/10.1080/02571862.2010.10639967

Meyer, J. H., Schumann, A. W., Wood, R. A., Nixon, D. J., & Van Den Berg, M. (2007). Recent advances to improve nitrogen use efficiency of sugarcane in the south African sugar industry. *Proceedings of the South African Sugar Technologists' Association*, *26*, 1–10.

Mualem, Y. (1976). A new model for predicting the hydraulic conductivity of unsaturated porous media. *Water Resources Research*, *12*, 513–522. https://doi.org/10.1029/WR012i003p00513

Nanteza, J., de Linage, C. R., Thomas, B. F., & Famiglietti, J. S. (2016). Monitoring groundwater storage changes in complex basement aquifers: An evaluation of the GRACE satellites over East Africa: GRACE groundwater dynamics in East Africa. *Water Resources Research*, *52*, 9542–9564. https://doi.org/10.1002/2016WR018846

Nasta, P., Szabó, B., & Romano, N. (2021). Evaluation of pedotransfer functions for predicting soil hydraulic properties: A voyage from regional to field scales across Europe. *Journal of Hydrology: Regional Studies*, *37*, 1–20. https://doi.org/10.1016/j.ejrh.2021.100903

Okamoto, K., Goto, S., Anzai, T., & Ando, S. (2021). Nitrogen leaching and nitrogen balance under differing nitrogen fertilization for sugarcane cultivation on a subtropical Island. *Water*, *13*, 1–13. https://doi.org/10.3390/w13050740

Otto, R., Castro, S. A. Q., Mariano, E., Castro, S. G. Q., Franco, H. C. J., & Trivelin, P. C. O. (2016). Nitrogen use efficiency for sugarcane-biofuel production: What is next? *Bioenergy Research*, *9*, 1272–1289. https://doi.org/10.1007/s12155-016-9763-x

Pidgeon, J. D. (1972). The measurement and prediction of available water capacity of Ferrallitic soils in Uganda. *Journal of Soil Science*, *23*, 431–441. https://doi.org/10.1111/j.1365-2389.1972.tb01674.x

Popp, J., Lakner, Z., Harangi-Rákos, M., & Fári, M. (2014). The effect of bioenergy expansion: Food, energy, and environment. *Renewable and Sustainable Energy Reviews*, *32*, 559–578. https://doi.org/10.1016/j.rser.2014.01.056

Premalatha, R. P., Bhakiyathu Saliha, B., Thiyageshwari, S., & Gurusamy, A. (2016). Influence of various sources and levels of fertilizers onnutrient use efficiencies of sugarcane. *Green Farming*, *7*, 1212–1215.

R Development Core Team. (2022). *A language and environment for statistical computing*. R Foundation for Statistical Computing, *7*, 1212–1215.

Ravishankara, A. R., Daniel, J. S., & Portmann, R. W. (2009). Nitrous oxide (N_2O): The dominant ozone-depleting substance emitted in the 21st century. *Science*, *326*, 123–125. https://doi.org/10.1126/science.1176985

Rawls, W. J., Brakensiek, D. L., & Saxtonn, K. E. (1982). Estimation of soil water properties. *Transactions of ASAE*, *25*, 1316–1320. https://doi.org/10.13031/2013.33720

Robinson, N., Brackin, R., Vinall, K., Soper, F., Holst, J., Gamage, H., Paungfoo-Lonhienne, C., Rennenberg, H., Lakshmanan, P., & Schmidt, S. (2011). Nitrate paradigm does not hold up for sugarcane. *PLoS ONE*, *6*, 1–9. https://doi.org/10.1371/journal.pone.0019045

Russo, T. A., Tully, K., Palm, C., & Neill, C. (2017). Leaching losses from Kenyan maize cropland receiving different rates of nitrogen fertilizer. *Nutrient Cycling in Agroecosystems*, *108*, 195–209. https://doi.org/10.1007/s10705-017-9852-z

Schaap, M. G., & Leij, F. J. (2000). Improved prediction of unsaturated hydraulic conductivity with the Mualem-van Genuchten model. *Soil Science Society of America Journal*, *64*, 843–851. https://doi.org/10.2136/sssaj2000.643843x

Schaap, M. G., Leij, F. J., & van Genuchten, M. T. (2001). Rosetta: A computer program for estimating soil hydraulic parameters with hierarchical pedotransfer functions. *Journal of Hydrology*, *251*, 163–176. https://doi.org/10.1016/S0022-1694(01)00466-8

Shishaye, H. A. (2015). Simulations of nitrate leaching from sugarcane farm in Metahara, Ethiopia, using the LEACHN model. *Journal of Water Resource and Protection*, *07*, 665–688. https://doi.org/10.4236/jwarp.2015.78055

Shukla, S. K., Yadav, R. L., Singh, P. N., & Singh, I. (2009). Potassium nutrition for improving stubble bud sprouting, dry matter partitioning, nutrient uptake and winter initiated sugarcane (*Saccharum* spp. hybrid complex) ratoon yield. *European Journal of Agronomy*, *30*, 27–33. https://doi.org/10.1016/j.eja.2008.06.005

Šimůnek, J., Genuchten, M. T., & Šejna, M. (2008). Development and applications of the HYDRUS and STANMOD software packages and related codes. *Vadose Zone Journal*, *7*, 587–600. https://doi.org/10.2136/vzj2007.0077

Singh, P., Suman, A., Tiwari, P., Arya, N., Gaur, A., & Shrivastava, A. K. (2008). Biological pretreatment of sugarcane trash for its conversion to fermentable sugars. *World Journal of Microbiology*

and Biotechnology, *24*, 667–673. https://doi.org/10.1007/s11274-007-9522-4

Soares, J. R., Cantarella, H., Vargas, V. P., Carmo, J. B., Martins, A. A., Sousa, R. M., & Andrade, C. A. (2015). Enhanced efficiency fertilizers in nitrous oxide emissions from urea applied to sugarcane. *Journal of Environmental Quality*, *44*, 423–430. https://doi.org/10.2134/jeq2014.02.0096

Stewart, L. K., Charlesworth, P. B., Bristow, K. L., & Thorburn, P. J. (2006). Estimating deep drainage and nitrate leaching from the root zone under sugarcane using APSIM-SWIM. *Agricultural Water Management*, *81*, 315–334. https://doi.org/10.1016/j.agwat.2005.05.002

Takeda, N., Friedl, J., Kirkby, R., Rowlings, D., De Rosa, D., Scheer, C., & Grace, P. (2022). Interaction between soil and fertiliser nitrogen drives plant nitrogen uptake and nitrous oxide (N_2O) emissions in tropical sugarcane systems. *Plant and Soil*, *477*, 647–663. https://doi.org/10.1007/s11104-022-05458-6

Takeda, N., Friedl, J., Rowlings, D., De Rosa, D., Scheer, C., & Grace, P. (2021). Exponential response of nitrous oxide (N_2O) emissions to increasing nitrogen fertiliser rates in a tropical sugarcane cropping system. *Agriculture, Ecosystems & Environment*, *313*, 107376. https://doi.org/10.1016/j.agee.2021.107376

Tamale, J., van Straaten, O., Hüppi, R., Turyagyenda, L. F., Fiener, P., & Doetterl, S. (2022). Soil greenhouse gas fluxes following conversion of tropical forests to fertilizer-based sugarcane systems in northwestern Uganda. *Agriculture, Ecosystems & Environment*, *333*, 1–13. https://doi.org/10.1016/j.agee.2022.107953

Tayade, A. S., Bhaskaran, A., & Anusha, S. (2020). IPNS–STCR-based nutrient management modules for enhancing soil health, fertilizer-use efficiency, productivity and profitability of tropical Indian sugarcane plant–ratoon agro-ecosystem. *Sugar Tech*, *22*, 32–41. https://doi.org/10.1007/s12355-019-00737-6

Thorburn, P. J., Biggs, J. S., Attard, S. J., & Kemei, J. (2011). Environmental impacts of irrigated sugarcane production: Nitrogen lost through runoff and leaching. *Agriculture, Ecosystems & Environment*, *144*, 1–12. https://doi.org/10.1016/j.agee.2011.08.003

Thorburn, P. J., Biggs, J. S., Palmer, J., Meier, E. A., Verburg, K., & Skocaj, D. M. (2017). Prioritizing crop management to increase nitrogen use efficiency in Australian sugarcane crops. *Frontiers in Plant Science*, *8*, 1–16. https://doi.org/10.3389/fpls.2017.01504

Thorburn, P. J., Wilkinson, S. N., & Silburn, D. M. (2013). Water quality in agricultural lands draining to the great barrier reef: A review of causes, management and priorities. *Agriculture, Ecosystems & Environment*, *180*, 4–20. https://doi.org/10.1016/j.agee.2013.07.006

Tilman, D., Cassman, K. G., Matson, P. A., Naylor, R., & Polasky, S. (2002). Agricultural sustainability and intensive production practices. *Nature*, *418*, 671–677. https://doi.org/10.1038/nature01014

Tomasella, J., & Hodnett, M. (2004). Pedotransfer functions for tropical soils. In *Developments in soil science* (pp. 415–429). Elsevier. https://doi.org/10.1016/S0166-2481(04)30021-8

Tomasella, J., & Hodnett, M. G. (1998). Estimating soil water retention characteristics from limited data in Brazilian Amazonia. *Soil Science*, *163*, 190–202. https://doi.org/10.1097/00010694-199803000-00003

Tombul, M., Akyürek, Z., & Ünal Sorman, A. (2004). Research note: Determination of soil hydraulic properties using pedotransfer functions in a semi-arid basin, Turkey. *Hydrology and Earth System Sciences*, *8*, 1200–1209. https://doi.org/10.5194/hess-8-1200-2004

van Genuchten, M. T. (1980). A closed-form equation for predicting the hydraulic conductivity of unsaturated soils. *Soil Science Society of America Journal*, *44*, 892–898. https://doi.org/10.2136/sssaj1980.03615995004400050002x

Van Looy, K., Bouma, J., Herbst, M., Koestel, J., Minasny, B., Mishra, U., Montzka, C., Nemes, A., Pachepsky, Y. A., Padarian, J., Schaap, M. G., Tóth, B., Verhoef, A., Vanderborght, J., Ploeg, M. J., Weihermüller, L., Zacharias, S., Zhang, Y., & Vereecken, H. (2017). Pedotransfer functions in earth system science: Challenges and perspectives. *Reviews of Geophysics*, *55*, 1199–1256. https://doi.org/10.1002/2017RG000581

Van Reeuwijk, L. P. (1993). Procedures for soil analysis. In *International soil Referene and information Centre (ISRIC)* (6th ed.). FAO.

Wang, W. J., Reeves, S. H., Salter, B., Moody, P. W., & Dalal, R. C. (2016). Effects of urea formulations, application rates and crop residue retention on N_2O emissions from sugarcane fields in Australia. *Agriculture, Ecosystems & Environment*, *216*, 137–146. https://doi.org/10.1016/j.agee.2015.09.035

Weynants, M., Vereecken, H., & Javaux, M. (2009). Revisiting Vereecken pedotransfer functions: Introducing a closed-form hydraulic model. *Vadose Zone Journal*, *8*, 86–95. https://doi.org/10.2136/vzj2008.0062

Wösten, J. H. M., Lilly, A., Nemes, A., & Le Bas, C. (1999). Development and use of a database of hydraulic properties of European soils. *Geoderma*, *90*, 169–185. https://doi.org/10.1016/S0016-7061(98)00132-3

Yadav, R. L. (2004). Enhancing efficiency of fertilizer n use in sugarcane by ring-pit method of planting. *Sugar Tech*, *6*, 169–171. https://doi.org/10.1007/BF02942719

Yang, L., Deng, Y., Wang, X., Zhang, W., Shi, X., Chen, X., Lakshmanan, P., & Zhang, F. (2021). Global direct nitrous oxide emissions from the bioenergy crop sugarcane (*Saccharum* spp. inter-specific hybrids). *Science of the Total Environment*, *752*, 1–12. https://doi.org/10.1016/j.scitotenv.2020.141795

Zhang, Y., & Schaap, M. G. (2019). Estimation of saturated hydraulic conductivity with pedotransfer functions: A review. *Journal of Hydrology*, *575*, 1011–1030. https://doi.org/10.1016/j.jhydrol.2019.05.058

Zhou, J., Gu, B., Schlesinger, W. H., & Ju, X. (2016). Significant accumulation of nitrate in Chinese semi-humid croplands. *Scientific Reports*, *6*, 1–8. https://doi.org/10.1038/srep25088

How to cite this article: Tamale, J., Nasta, P., Doetterl, S., Hutson, J., van Straaten, O., Turyagyenda, L. F., & Fiener, P. (2024). Impact of urea fertilization rates on nitrogen losses, productivity and profitability in East African sugarcane plantations. *Soil Use and Management*, *40*, e13030. https://doi.org/10.1111/sum.13030

APPENDIX A

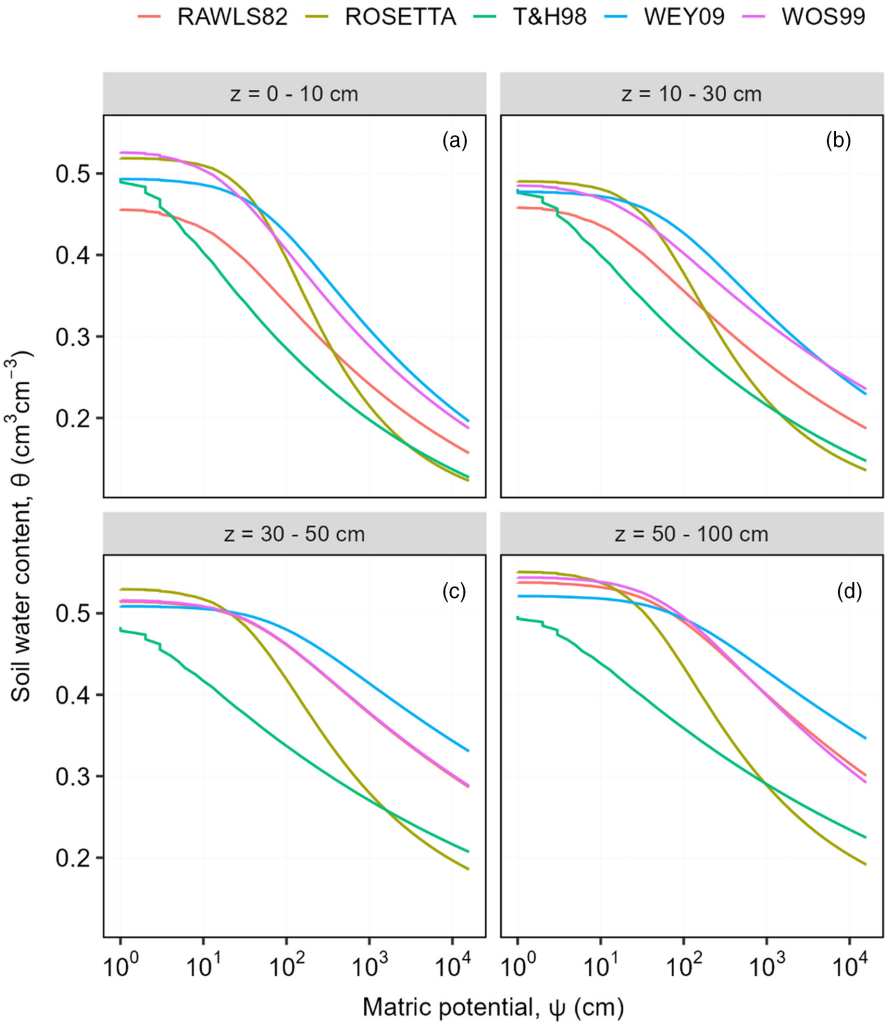

FIGURE A1 Soil water retention curves at four different soil depths (0–10 cm—a; 10–30 cm—b; 30–50 cm—c and 50–100 cm—d) based on soil hydraulic parameters of the van Genuchten model (θ_r, θ_s, α and n) estimated using five PTFs (RAWLS82, ROSETTA, T&H98, WEY09 and WOS99).

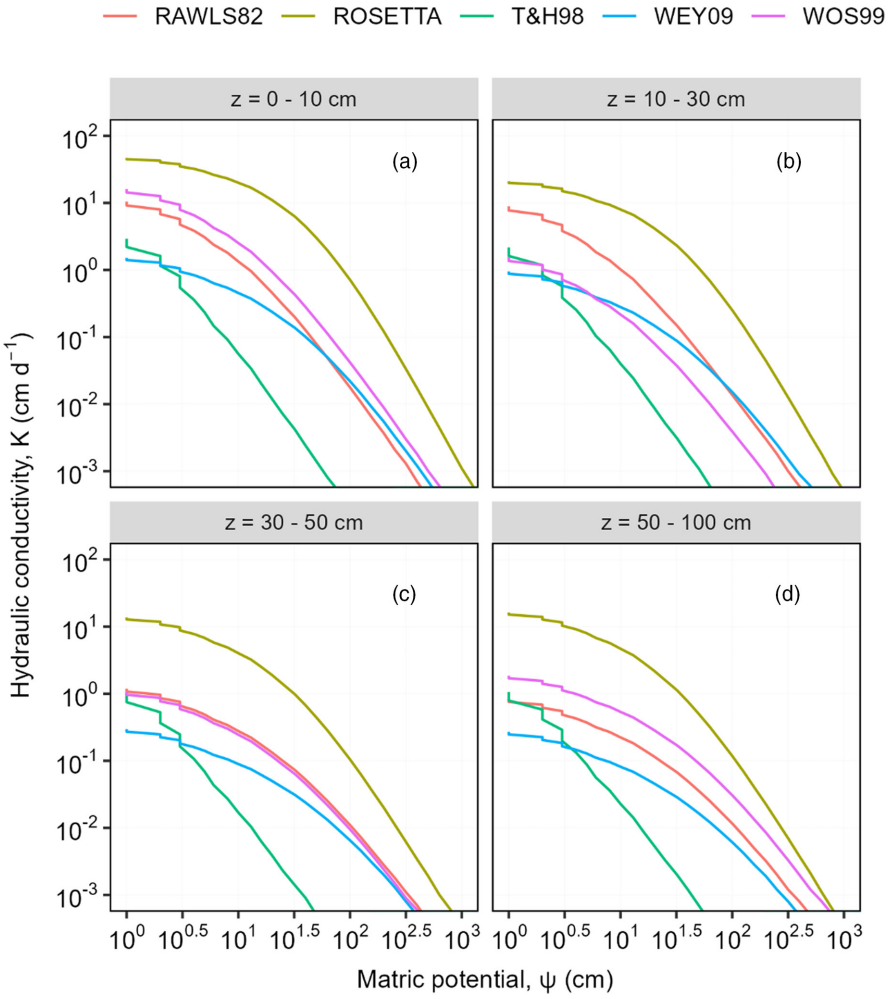

FIGURE A2 Soil hydraulic conductivity curves at four different soil depths (0–10 cm—a; 10–30 cm—b; 30–50 cm—c and 50–100 cm—d) based on soil hydraulic parameters of the van Genuchten model (θ_r, θ_s, α and n) and saturated hydraulic conductivity, K_s, estimated using five PTFs (RAWLS82, ROSETTA, T&H98, WEY09 and WOS99).

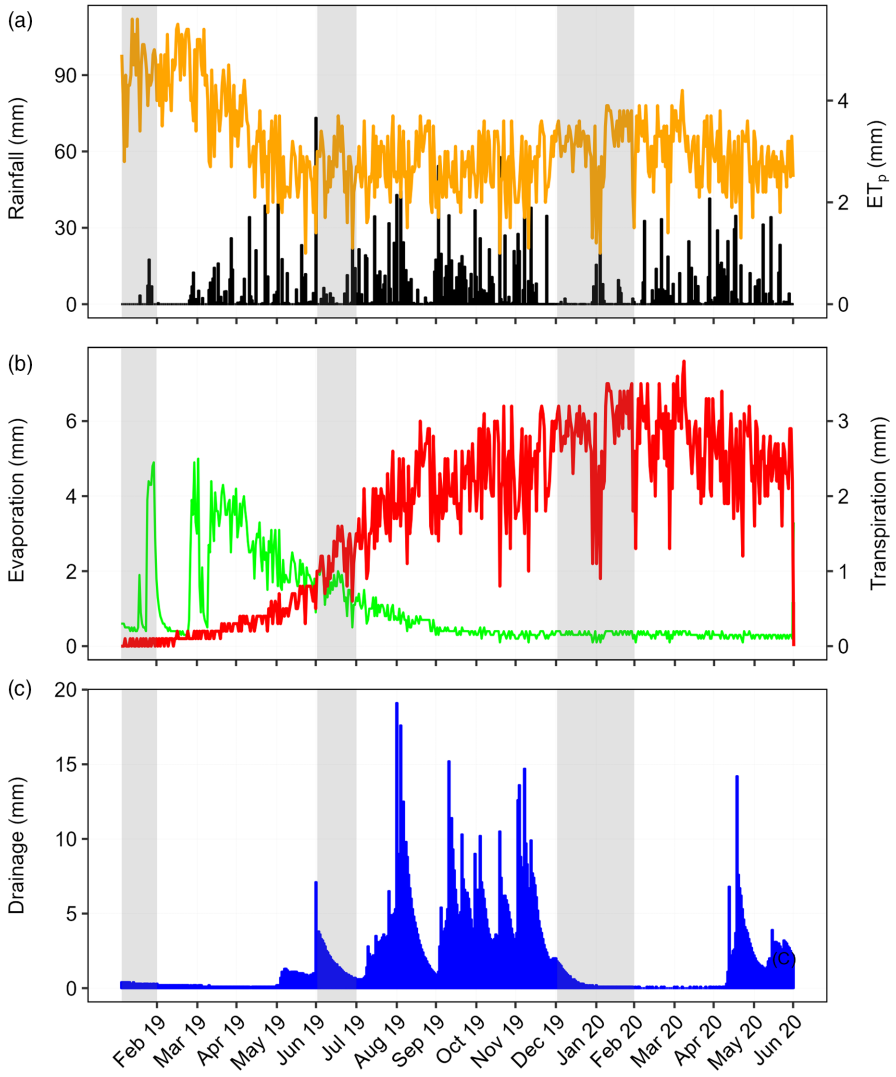

FIGURE A3 Panel a shows daily rainfall (cm; measured with ATMOS41 weather station, black bars) and potential evapotranspiration (ET_p; cm, brown line), estimated with the Penman–Monteith approach (Allen et al., 1998), panel b shows modelled evaporation (cm, green line) and actual transpiration (cm, red line) and panel c shows average modelled drainage (cm, blue bars) between February 2019 and June 2020 based on ROSETTA; RAWLS82 and WOS99 PTFs. The grey-shaded rectangles in panels a, b and c represent the lengths of dry periods in 2019 and 2020.

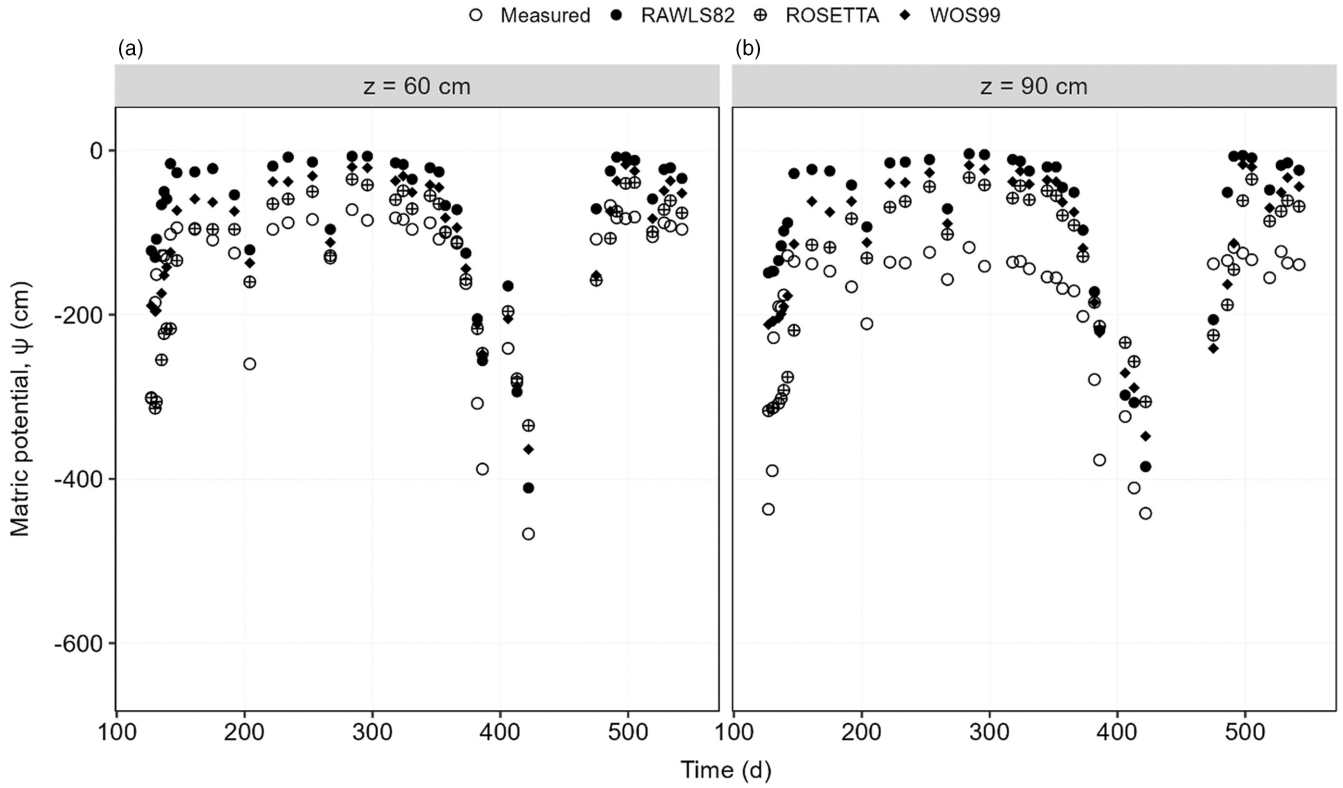

FIGURE A4 Predicted matric potential with ROSETTA, RAWLS82 and WOS99 PTFs and the measured soil matric potential at soil depths of 60 (a) and 90 cm (b) between May 2019 and June 2020.

TABLE A1 List of equations featuring in the five PTFs used to estimate the soil hydraulic parameters of the van Genuchten (1980) soil water retention function and saturated hydraulic conductivity (θ_r, θ_s, α and n).

RAWLS82

Rawls et al. (1982) developed 12 regression equations to relate soil water content values to prescribed soil matric head values by using the following general equation:

$$\theta(\psi) = a + b\,Sa + c\,Si + d\,Cl + e\,SOC + f\,\rho_b \quad \text{(A1)}$$

where a, b, c, d, e and f are the regression coefficients reported in Table A2.

The data pairs, $\theta(\psi)$ were fitted to the van Genuchten water retention curve to optimize its four parameters (θ_r, θ_s, α and n).

Saturated hydraulic conductivity, K_s (cm d^{-1}), was estimated by using the empirical equation proposed by Guarracino (2007):

$$K_s = 4.65 \bullet 10^4 \theta_s \alpha^2 \quad \text{(A2)}$$

ROSETTA

ROSETTA was developed by Schaap et al. (2001). It is based on artificial neural network analysis (Zhang and Schaap, 2019) and implemented in HYDRUS-1D, where the five empirical van Genuchten (1980) model parameters (θ_r, θ_s, α and n) can be derived from measurements of sand, silt, clay, organic matter and bulk density.

T&H98

Tomasella and Hodnett (1998) developed nine regression equations to relate soil water content (θ) values to prescribed soil matric head (ψ) values by using the following general equation:

$$\theta(\psi) = 0.01\,(a\,SOC + b\,Si + c\,Cl + d) \quad \text{(A3)}$$

where a, b, c and d are the regression coefficients reported in Table A3.

The data pairs, $\theta(\psi)$ were fitted to the van Genuchten water retention curve to optimize its four parameters (θ_r, θ_s, α and n).

Saturated hydraulic conductivity, K_s (cm d^{-1}), was estimated by using the empirical equation proposed by Guarracino (2007) (Equation A2).

WEY09

$$\theta_s = 0.6355 + 0.0013 * \mathrm{Cl} - 0.1631 * \rho_b \quad \text{(A4)}$$

$$\theta_r = 0 \quad \text{(A5)}$$

$$\alpha = \exp(-4.3003 - 0.0097 * \mathrm{Cl} + 0.0138 * \mathrm{Sa} - 0.0992 * \mathrm{SOC}) \quad \text{(A6)}$$

$$n = \exp\left(-1.0846 - 0.0236 * \mathrm{Cl} - 0.0085 * \mathrm{Sa} + 1.3699 * 10^{-4} * \mathrm{Sa}^2\right) + 1 \quad \text{(A7)}$$

$$m = 1 - \frac{1}{n} \quad \text{(A8)}$$

Saturated hydraulic conductivity, K_s (cm d^{-1}), was estimated by using the empirical equation proposed by Guarracino (2007) (Equation A2).

WOS99

$$\theta_s = 0.7919 + 0.001691 * \mathrm{Cl} - 0.29619 * \rho_b - 0.000001491 * \mathrm{Si}^2 + 0.0000821 * \mathrm{SOM}^2 + \frac{0.02427}{\mathrm{Cl}} + \frac{0.01113}{\mathrm{Si}} + 0.01472 * \ln(\mathrm{Si}) - 0.000073 * \mathrm{SOM} * \mathrm{Cl} - 0.000619 * \rho_b * \mathrm{Cl} - 0.001183 * \rho_b * \mathrm{SOM} - 0.0001664 * \mathrm{topsoil} * \mathrm{Si} \quad \text{(A9)}$$

$$\theta_r = 0 \quad \text{(A10)}$$

$$\alpha = \exp\left(-14.96 + 0.03135 * \mathrm{Cl} + 0.0351 * \mathrm{Si} + 0.646 * \mathrm{SOM} + 15.29 * \rho_b - 0.192 * \mathrm{topsoil} - 4.671 * {\rho_b}^2 - 0.000781 * \mathrm{Cl}^2 - 0.00687 * \mathrm{SOM}^2 + \frac{0.0449}{\mathrm{SOM}} + 0.0663 * \ln(\mathrm{Si}) + 0.1482 * \ln(\mathrm{SOM}) - 0.04546 * \rho_b * \mathrm{Si} - 0.4852 * \rho_b * \mathrm{SOM} + 0.00673 * \mathrm{topsoil} * \mathrm{Cl}\right) \quad \text{(A11)}$$

$$n = 1 + \exp\left(-25.23 - 0.02195 * \mathrm{Cl} + 0.0074 * \mathrm{Si} - 0.1940 * \mathrm{SOM} + 45.5 * \rho_b - 7.24 * {\rho_b}^2 + 0.0003658 * \mathrm{Cl}^2 + 0.002885 * \mathrm{SOM}^2 - \frac{12.81}{\rho_b} - \frac{0.1524}{\mathrm{Si}} - \frac{0.01958}{\mathrm{SOM}} - 0.2876 * \ln(\mathrm{Si}) - 0.0709 * \ln(\mathrm{SOM}) - 44.6 * \ln(\rho_b) - 0.02264 * \rho_b * \mathrm{Cl} + 0.0896 * \rho_b * \mathrm{SOM} + 0.00718 * \mathrm{topsoil} * \mathrm{Cl}\right) \quad \text{(A12)}$$

$$m = 1 - \frac{1}{n} \quad \text{(A13)}$$

$$K_s = \exp\left(7.755 + 0.0352 * \mathrm{Si} + 0.93 * \mathrm{topsoil} - 0.967 * (\rho_b)^2 - 0.00048 * \mathrm{Cl}^2 - 0.000322 * \mathrm{Si}^2 + \frac{0.001}{\mathrm{Si}} - \frac{0.0748}{\mathrm{SOM}} - 0.643 * \ln(\mathrm{Si}) - 0.01398 * \rho_b * \mathrm{Cl} - 0.1673 * \rho_b * \mathrm{SOM} + 0.02986 * \mathrm{topsoil} * \mathrm{Cl} - 0.03305 * \mathrm{topsoil} * \mathrm{Si}\right) \quad \text{(A14)}$$

Note: Input data are sand (*Sa*; %), silt (*Si*; %), clay (*Cl*; %), soil organic matter (SOM; %) and bulk density (ρ_b; g cm^{-3}). Soil organic carbon (*SOC*; %) is obtained as *SOC* = *SOM*/1.724 and *topsoil* = 1 if soil samples were collected in the uppermost soil layer or *topsoil* = 0 if soil samples were collected in the deeper layers of the soil profile. The equations are reproduced from Nasta et al. (2021).

TABLE A2 Tabulated regression coefficients (a, b, c, d, e, and f) in Equation A1 to predict the soil water content (θ) values associated with 12 prescribed soil matric head values (ψ).

ψ (cm)	a	b	c	d	e	f
−40	0.790	−0.00370	0	0	0.0100	−0.132
−70	0.714	−0.00300	0	0.00170	0	−0.169
−100	0.412	−0.00300	0	0.00230	0.0317	0
−200	0.312	−0.00240	0	0.00320	0.0314	0
−330	0.258	−0.00200	0	0.00360	0.0299	0
−600	0.207	−0.00160	0	0.00400	0.0275	0
−1000	0.0349	0	0.00140	0.00550	0.0251	0
−2000	0.0281	0	0.00110	0.00540	0.0200	0
−4000	0.0238	0	0.000800	0.00520	0.0190	0
−7000	0.0216	0	0.000600	0.00500	0.0167	0
−10,000	0.0205	0	0.000500	0.00490	0.0154	0
−15,000	0.0260	0	0	0.00500	0.0158	0

TABLE A3 Tabulated regression coefficients (a, b, c, and d) in Equation A3 to predict the soil water content (θ) values associated with nine prescribed soil matric head (ψ) values.

ψ (cm)	a	b	c	d
−1	2.24	0.298	0.159	37.9
−10	0	0.530	0.255	23.8
−30	0	0.552	0.262	18.5
−60	0	0.576	0.300	12.3
−100	0	0.543	0.321	9.81
−330	0	0.426	0.404	4.05
−1000	0	0.369	0.351	3.20
−5000	0	0.258	0.361	1.57
−15,000	0	0.150	0.396	0.91